



**Iam Kim de Souza Hermont**

**Robust Adaptive Algorithms Applied to  
Active Noise Cancellation**

**Dissertação de Mestrado**

Thesis presented to the Programa de Pós-graduação em Engenharia Elétrica, do Departamento de Engenharia Elétrica da PUC-Rio in partial fulfillment of the requirements for the degree of Mestre em Engenharia Elétrica.

Advisor : Prof. Rodrigo Caiado de Lamare  
Co-advisor: André Robert Flores Manrique

Rio de Janeiro  
August 2024



**Iam Kim de Souza Hermont**

**Robust Adaptive Algorithms Applied to  
Active Noise Cancellation**

Thesis presented to the Programa de Pós-graduação em Engenharia Elétrica da PUC-Rio in partial fulfillment of the requirements for the degree of Mestre em Engenharia Elétrica. Approved by the Examination Committee:

**Prof. Rodrigo Caiado de Lamare**

Advisor

Departamento de Engenharia Elétrica – PUC-Rio

**André Robert Flores Manrique**

Co-advisor

Departamento de Engenharia Elétrica – PUC-Rio

**Profa. Mariane Rembold Petraglia**

UFRJ

**Prof. Amaro Azevedo Lima**

CEFET-RJ

**Prof. Lukas Tobias Nepomuk Landau**

Departamento de Engenharia Elétrica – PUC-Rio

Rio de Janeiro, August 27th, 2024

All rights reserved.

### **Iam Kim de Souza Hermont**

The author graduated in Acoustical Engineering from the Universidade Federal de Santa Maria (UFSM), in Santa Maria/RS, Brazil, 2018

#### Bibliographic data

Hermont, Iam Kim de Souza

Robust Adaptive Algorithms Applied to Active Noise Cancellation / Iam Kim de Souza Hermont; advisor: Rodrigo Caiado de Lamare; co-advisor: André Robert Flores Manrique. – 2024.

79 f: il. color. ; 30 cm

Dissertação (mestrado) - Pontifícia Universidade Católica do Rio de Janeiro, Departamento de Engenharia Elétrica, 2024.

Inclui bibliografia

1. Engenharia Elétrica – Teses. 2. Filtragem adaptativa. 3. Métodos de processamento robustos. 4. Cancelamento ativo de ruído. 5. Processamento de sinais de áudio. 6. Acústica. I. de Lamare, Rodrigo. II. Manrique, André. III. Pontifícia Universidade Católica do Rio de Janeiro. Departamento de Engenharia Elétrica. IV. Título.

CDD: 621.3

To my mom, dad, bro, and fellas  
for the basis, support and encouragement.

## Acknowledgments

Firstly, my gratitude to my mother Catherine, my father José Henrique, and my brother Yuri, because without my family I wouldn't have had the same foundation, support, and reference.

To my supervisor Professor Rodrigo, thank you for all your support and advice, which was fundamental to completing this work. To my co-supervisor André, for his companionship and help, which was essential for me to carry out this research.

To my friend Cris, who welcomed me to Rio de Janeiro from day one and whose home and important moments we shared for most of this journey, "I'm just grateful". To my friends and family who cheered me on and were there for me in some way during this master's degree.

I would like to thank my colleagues at PUC-Rio, Ana, Francisco, and Deja, among other students and workers, with whom, between corridors and elevators, we shared the routine, ideas, and coffee, smoothing out the rush of life together. Téo, Elaine, and Ballisteri thank you so much to these "guardian angels" whose collaboration in the processes related to this master's degree was of the utmost importance.

To my laboratory colleagues Angelo, Tonny, Hassan, Roberto, Alireza, Saeed, Reencarnación, Mary Ann, Nayyab, and Lu. Thank you for all the cultural experiences of their places and all the moments of dialog about science and life.

To professors Marco Grivet, Karla Figueiredo, Marley Vellasco, and Alan Kubrusly, thanks for their considerations, lessons, and shared knowledge.

To the professors who took part in the examining committee, Mariane Petraglia, Amaro Lima, and Lukas Landau, thanks for their review and contributions to this paper.

Finally, I would like to pay my respects to CNPq and FAPERJ for their support in this mastering research. This study was financed in part by the Coordenação de Aperfeiçoamento de Pessoal de Nível Superior – Brasil (CAPES) – Finance Code 001.

## Abstract

Hermont, Iam Kim de Souza; de Lamare, Rodrigo (Advisor); Manrique, André (Co-Advisor). **Robust Adaptive Algorithms Applied to Active Noise Cancellation**. Rio de Janeiro, 2024. 79p. Dissertação de Mestrado – Departamento de Engenharia Elétrica, Pontifícia Universidade Católica do Rio de Janeiro.

The well-known adaptive algorithm called least-mean square (LMS) is a simple and efficient approach to active noise cancellation application problems. However, in the presence of non-Gaussian noises or non-linear environments, the standard LMS commonly cannot reach satisfactory performance. Therefore, a wide range of robust adaptive processing techniques have been investigated in the last few decades. This thesis proposes a robust adaptive filtering approach for noise cancellation. In particular, the model uses the classical filtered-X framework with the developed method in this research, it is based on hyperbolic tangent exponential generalized Kernel M-estimator function (HEKM), which achieves optimal performance in terms of Average Noise Reduction (ANR). The results demonstrate the cost-effectiveness of the proposed algorithm in suppressing spurious noises in different input systems.

## Keywords

Adaptive filtering; Robust processing methods; Active noise cancellation; Audio signal processing; Acoustics.

## Resumo

Hermont, Iam Kim de Souza; de Lamare, Rodrigo; Manrique, André. **Algoritmos Adaptativos Robustos Aplicados ao Cancelamento Ativo de Ruído**. Rio de Janeiro, 2024. 79p. Dissertação de Mestrado – Departamento de Engenharia Elétrica, Pontifícia Universidade Católica do Rio de Janeiro.

O conhecido algoritmo adaptativo denominado *least-mean square* (LMS) é uma abordagem simples e eficiente para problemas de cancelamento ativo de ruído (ANC). No entanto, na presença de sinais não Gaussianos ou sistemas não lineares, o clássico LMS comumente não alcança um desempenho satisfatório. Por essa razão, um amplo número de técnicas de processamento de sinais adaptativo robustas tem sido investigadas nas últimas décadas. Essa dissertação propõe uma abordagem de filtragem adaptativa robusta para cancelamento ativo de ruído. Em particular, o modelo utiliza a clássica estrutura *filtered-X* junto ao método desenvolvido neste trabalho, baseado na derivação de uma função tangente hiperbólica exponencial kernel generalizado M-estimador (HEKM), o qual alcançou um desempenho ótimo em termos da Redução de Ruído Média (ANR). Os resultados demonstraram o custo-benefício do algoritmo proposto para supressão de diferentes tipos de sinais espúrios na entrada do sistema.

## Palavras-chave

Filtragem adaptativa; Métodos de processamento robustos; Cancelamento ativo de ruído; Processamento de sinais de áudio; Acústica.

## Table of contents

<b>1</b>	<b>Introduction</b>	<b>14</b>
1.1	Motivation	15
1.2	Contributions	16
1.3	Dissertation Outline	16
1.4	List of Publications	17
1.5	Notation	17
<b>2</b>	<b>Active Noise Cancellation Review</b>	<b>19</b>
2.1	Adaptive Filtering Fundamentals	21
2.2	Robust Filtering Methods	31
2.3	Statistical Analysis	33
2.4	Summary	38
<b>3</b>	<b>Hyperbolic Exponential Kernel M-estimate Algorithm</b>	<b>39</b>
3.1	System modeling	39
3.2	Derivation of the Proposed FXHEKM Algorithm	41
3.3	Statistical Analysis	47
3.4	Numerical Results	57
<b>4</b>	<b>Conclusions and Future Work</b>	<b>73</b>
<b>5</b>	<b>Bibliography</b>	<b>75</b>

## List of figures

Figure 2.1	Diagram of a generic feedforward ANC system.	20
Figure 2.2	Block diagram of an Adaptive Filter.	22
Figure 2.3	3D MSE performance surface (case $L = 2$ ).	24
Figure 2.4	Block diagram of an LMS adaptive filter framework.	28
Figure 2.5	Diagram of FXLMS frameworks: (a) feedforward; (b) feedback.	31
Figure 2.6	Diagram of the feedforward FXLMS NLANC model.	32
Figure 3.1	Block diagram of the proposed Adaptive Noise Cancellation system.	40
Figure 3.2	Objective function of HEKM related to the parameter $\alpha$ .	42
Figure 3.3	Objective function of HEKM related to the parameter $p$ .	42
Figure 3.4	Objective function of HEKM related to the parameter $\eta$ .	43
Figure 3.5	Derivative of objective function get the FXHEKM related to the set of parameter $\alpha$ .	44
Figure 3.6	Derivative of objective function get the FXHEKM related to the set of parameter $p$ .	45
Figure 3.7	Derivative of objective function get the FXHEKM related to the set of parameter $\eta$ .	46
Figure 3.8	Computational Complexity of the algorithms approached.	58
Figure 3.9	Analysis of the initial system identification realized to defined estimation of the secondary path $\hat{S}(z)$ to $\alpha = 2.0$ (case 1).	60
Figure 3.10	Analysis of the initial system identification realized to defined estimation of the secondary path $\hat{S}(z)$ to $\alpha = 1.5$ (case 2).	61
Figure 3.11	MSE comparison between HEKM method approaches for Gaussian distribution noise (SNR = 20 dB).	62
Figure 3.12	MSE comparison between HEKM method approaches for Gaussian distribution noise (SNR = 10 dB).	63
Figure 3.13	MSE comparison between HEKM method approaches for Gaussian distribution noise (SNR = 3 dB).	64
Figure 3.14	MSE analysis between different SNR values of the standard HEKM method for Gaussian distribution noise.	64
Figure 3.15	MSE comparison between HEKM method approaches for Gaussian distribution noise ( $\alpha - Stable = 2.0$ ).	65
Figure 3.16	MSE comparison between HEKM method approaches for Gaussian distribution noise ( $\alpha - Stable = 2.0$ ).	66
Figure 3.17	MSE comparison between HEKM method approaches for Gaussian distribution noise (SNR = 20 dB).	67
Figure 3.18	ANR comparison between HEKM approaches for Gaussian distribution noise (SNR = 20 dB).	68
Figure 3.19	ANR comparison between HEKM method approaches for Gaussian distribution noise (SNR = 10 dB).	68
Figure 3.20	ANR comparison between HEKM method approaches for Gaussian distribution noise (SNR = 3 dB).	69
Figure 3.21	ANR comparison between HEKM method against other classical/robust approaches for Gaussian distribution noise (SNR = 20 dB).	70

Figure 3.22 ANR comparison between HEKM approaches for impulsive noise ( $\text{SNR} \approx 25\text{dB}$ ).	70
Figure 3.23 ANR comparison between HEKM method against other classical/robust approaches for Gaussian distribution noise ( $\text{SNR} \approx 25\text{dB}$ ).	71

## List of tables

Table 2.1	Steps to deploy the LMS algorithm.	28
Table 3.1	Computation Complexity of some algorithms per iteration.	58

## List of Abbreviations

ANC – *Active Noise Cancellation/Control*

ANR – *Average Noise Reduction*

FX – *filtered-X* structure

FXEHCF – *Filtered-X Exponential Hyperbolic Cosine Function* model

FXGHT – *Filtered-X Generalized Hyperbolic Tangent* model

FXGMCC – *Filtered-X Generalized Maximum Correntropy Criteria* model

FXGR – *Filtered-X General Robust* model

FXHEKM – *Filtered-X Hyperbolic Exponential Kernel M-Estimator* model

FXLMS – *Filtered-X Least Mean Square* model

GD – *Gradient Descent* method

HEKM – *Hyperbolic Exponential Kernel M-Estimator* function

IFXGMCC – *Improved FXGMCC* model

LMS – *Least Mean Square* algorithm

MMSE – *Minimum Mean-Square Error* Estimator

MSE – *Mean Squared Error* Estimator

NC – *Noise Cancelling/Control*

SNR – *Signal-to-Noise Ratio*

*It's not who you are that holds you back,  
it's who you think you are not.*

**Jean-Michel Basquiat, 1960-1988.**

# 1

## Introduction

One important research application in the audio signal processing field is related to control and/or canceling undesired acoustic signals in the environment, which are usually known as *noise*. In real applications, different noise sources degrade heavily the general operation of a system. Therefore, noise reduction (NR) approaches are fundamental to guarantee an appropriate performance. To this end, electronic systems capable of canceling different sources of interference, vibration, and reverberation have been designed and developed in the last 80 years [1].

To improve the range of this noise suppression structures, the computational approaches using smart digital signal processing algorithms came to enhance the capacity and efficiency of the system's response [2, 3]. Based on this engineering concept, *Active Noise Cancellation* (ANC) has emerged as a powerful technology for attenuating the level of noise in a series of electromechanical or electroacoustic networks [4]. Into the development of the electronic systems that boosted the high-performance DSP devices and algorithms, at least since the 80s and even with the development of the Artificial Intelligence (AI) and other areas, the whole subject of the ANC frameworks are the case study and applicable technique in expansion [5].

According to Haykin [6], active noise control is an effective way to reduce the noise level in electroacoustic or electromechanical systems. In other words, it is a framework whose function is to control the noise that affects a system. This task is achieved through an adaptive algorithm that calculates the optimum solution, and through the electro-mechanical-acoustic hardware that applies the solution in the secondary propagation path in order to cancel out the noise of this environment.

This curious and interesting kind of “sound control methodology”, is reached by introducing an *antinoise* wave through an appropriate segment of secondary sources [7, 8]. Specifically, an adaptive algorithm obtains the cancelling signal and an electro-mechanical-acoustic system propagates that wave with the same amplitude and inverse phase through the secondary path, thus achieving the cancellation of noise in the observed environment [7, 9].

One of the most well-known adaptive methods in history is the *Least Mean Square* (LMS) algorithm, created by Ted Hoff and Bernard Widrow, brings a new point of view at the time for the improvement of adaptive learning approaches, *e.g.* the stochastic gradient descent applied in adaptive filtering

(*vide* Widrow et al [10]) or the delta rule in neural networks.

With the LMS method, it was enabled to learn about the statistical behaviour of the signal through adaptive processing. This adaptive process involves the computation of the error between the desired and output signals. Then, the error is used by the adaptive algorithm to update the parameters of the filter. This acknowledged algorithm is so simple and stable for linear systems and noises of Gaussian behavior [11], that it was studied and used for decades in ANC arrangements beyond other many applications.

Unifying the classic adaptive algorithm named LMS with another renowned framework approach, that uses an auxiliary path, called *filtered-X* [11], the result is a powerful combination known as FXLMS<sup>1</sup>.

However, in some specific cases like nonlinear structures (*e.g* chaotic, unpredictable) or noises with nature non-Gaussian (impulsive, cosine, complex signals or with additive noise), the accuracy of the FXLMS usually degrades. For this reason, some methodology that takes into account the stochastic characteristics of the signal must be adopted, thus making the treatment of the physical features of this signals and its systems involved feasible [12]. In this study, the mathematical basis of the objective function, adaptive learning, and statistical analysis of the algorithm will be addressed.

In general, to deal with this type of problem throughout history, a lot of different concepts were created using engineering tools and generating a series of signal processing frameworks, based on a range of problems and the complex signals that are needed to apply noise reduction [13]. These facts compose a huge scenario that proves that this area still has scientific potential to keep on growing and to contribute technologically to real-world problems related to ANC and other fields.

## 1.1 Motivation

Over the years, some techniques have been employed to deal with the wide range of problems in ANC systems, such as the well-known variable step-size [14], the regularized least-squares method [15], least mean  $p$ -power [16]. Heuristic methods such as particle swarm optimization [17] or different methods of the objective function optimization like stochastic gradient descent, Newton [18] and  $q$ -gradient [19] (*vide* the survey at Lu Lu *et al* [12,13]), Kernel Adaptive Filtering approaches [20] etc. They are some of the perspectives

<sup>1</sup>*vide* the history of the method in “*History, applications, and subsequent development of the FXLMS Algorithm, IEEE Signal Processing Magazine Vol. 30, May 2013.*”

researched in a universe of possibilities when the focus is to seek the best solution for this classical problem.

Another set of key ideas were concerned with the consideration of different types of objective functions used to develop robust algorithms using methods like the correntopy criterion [21]; hyperbolic trigonometric functions [22, 23] and an exponential conjugated version [24]; the M-estimator method [25] and others.

Last but not least, on the contrary, one of the most important reasons for this area of study is a wide range of related areas to ANC which benefit from the development of adaptive filtering devices in signal processing, such as noise reduction, system identification, echo cancellation, signal estimation, pattern recognition, etc. [5] in many different areas, such as medicine, communications, water treatment, among others [26].

The motivation of this work based on the research of a novel algorithmic model, which count the state-of-the-art in adaptive filtering methods, reaching a robust approach able to lead with some scenarios in the active noise cancellation.

## 1.2

### Contributions

The contributions of this thesis can be summarized into:

- An active noise cancellation framework, composed by a filtered-X ANC structure and robust adaptive filtering algorithm, using a novel approach called FXHEKM. This methodology can work as well with Gaussian and non-Gaussian (*e.g.* pseudo impulsive  $\alpha$ -Stable distribution) noises, it reaching a high performance with stable results;
- A comprehensive statistical analysis of the FXHEKM adaptive processing algorithm. This analysis comprehends the objective function derivation and other statistical aspects such as stability, convergence as well as the important evaluation metrics like computational cost, MMSE and ANR;

## 1.3

### Dissertation Outline

This dissertation is structured as follows:

- In Chapter 2, we present a literature review of the active noise cancellation problem and related topics, that is fundamental for the reader

to conceptual understand about: adaptive filtering techniques; active noise cancellation systems; stability and convergence analysis; and robust methods employed in this kind of problems, which obtain best performance approach in terms of noise suppression results.

- Chapter 3 details the development of the proposed FXHEKM algorithm. In particular, the proposed FXHEKM algorithm is described in detail including: the system modeling; the mathematical derivation of the proposed FXHEKM algorithm; the statistical analysis, including the stability and MSE analysis along with numerical simulations, that are devised to verify the algorithm performance and its implications. Moreover, the analytically simulated results are presented to evaluate, prove and discuss about the performance among other interesting issue of the proposed model.
- Chapter 4 brings the final considerations about the work with conclusions, important notes and possible future works that would be extensions of this research.

## 1.4

### List of Publications

The results of the research work are published in the papers listed as follows:

Conference Paper:

- I. K. de S. Hermont, A. R. Flores and R.C. de Lamare, “Robust Adaptive Filtering Based on the Hyperbolic Tangent Exponential Kernel M-Estimator Function for Active Noise Cancellation”, IEEE International Symposium on Wireless Communication Systems (ISWCS), Rio de Janeiro, Brazil, 2024.

## 1.5

### Notation

$\mathbf{x}(n)$	vector (bold lower case letters)
$\mathbf{x}'(n), \mathbf{s}'(n)$	filtered-X response/secondary path estimation
$\hat{J}(n)$	estimation of objective function
$\mathbf{R}$	matrix (bold upper case letters)
$\mathbf{I}$	identity matrix
$E[\cdot]$	expected value operator

$\  \cdot \ _2^2$	$l_2$ – norm operator
$\exp(\cdot)$	exponential function
$\tanh(\cdot), \operatorname{sech}(\cdot), \operatorname{cosh}(\cdot)$	hyperbolic trigonometric functions
$\mu, \xi, \eta$	constant value parameters

## 2

### Active Noise Cancellation Review

Over the last 50 years, there has been a growing interest in active techniques for sound control. Although many physical principles of sound control were established during this time, the technology to implement *active noise control* successfully has only become available recently. In fact, modern approaches employ advanced signal processing methods to exploit the acoustic aspects of the problem [27].

*Active noise control*, most known as *active noise cancellation* (ANC), refers to the concept of obtaining suppression of noise by introducing a system to recognize and apply an “anti-noise” wave through an appropriate array of secondary sources [28]. As referred to by Nelson and Elliott [27], the ANC topic emerged in the last century as a promising field of engineering, research and development, and it continues improving through novel formulations and new problems with their recent solutions.

Utilized in many applications where is necessary the control and attenuation of noise in a wide range of modern dynamic systems, the models of ANC were developed with several technical approaches and employ engineering and other scientific and technological areas.

It is worth mentioning the fundamental contributions of Paul Lueg with the *Process of silencing sound oscillations* in 1936 [29] where his pioneer patent brings a preliminary understanding about the area in the engineering point-of-view. In the article *Electronic Control of Noise, Vibration, and Reverberation* in 1956 [30], Olson and May gives a first formal and preliminary mathematical approach to the ANC field. Another important contribution came through Hoff in his PhD work, which was advised by Bernard Widrow and developed the well-known LMS algorithm in 1960 [31] among other important names who contributed in the literature, research and practical aspects of the area.

The secondary path can be interpreted as the environment by which is transmitted the computed signal of the adaptive filter (*vide* Section 2.1). This filtered response is passed on to the output, where the residual error is calculated between the desired signal and filter output, in order to found the value of the estimation difference to update the filter parameters to the next iteration of the algorithm.

In general, there are two principal types of systems: the first one is called *feedforward* system, as shown in Figure 2.1. The second one is known as *feedback* system, where the term feedback refers to the idea of the existence of an acoustic return path of propagation and consequently, a delay in the environment. Due to the fact that there is only one sensor at the output to calculate the error based on the measure of input and response, there is an intrinsic feedback phenomenon in the system.

In Figure 2.1, we can see that from a Noise Source (known or not) the Reference Microphone picks up the input signal  $x(n)$  (from Primary Noise), while the second one picks up the residual error microphone signal  $e(n)$  (by Error Microphone). Both values are fed into the ANC system, which after computation applies a suppression signal by means of the filtered value  $y(n)$  to the speaker output. The aim is to achieve an output response that cancels out the signal in the primary noise path and to zero out the residual error value via an iterative process.

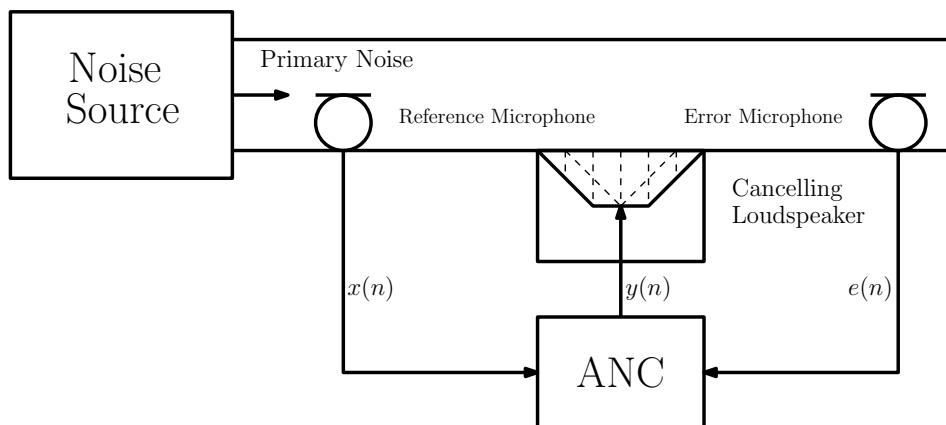


Figure 2.1: Diagram of a generic feedforward ANC system.

As described in more detail in Section 2.1.4, in this work we chose the feedforward structure due to its more general theoretical understanding and broader field of application. In the subsequent sections of Chapter 2, we will cover some fundamental knowledge for dealing with ANC systems.

## 2.1

### Adaptive Filtering Fundamentals

The ANC field would not have developed in the same way without the contribution of the mathematical approaches and the algorithms of adaptive signal processing. Adaptive filters have received considerable attention in the last five decades and is still developed by many researchers around the world, which are responsible for innovations in algorithms and frameworks adopted in ANC and other areas. Using an implementation architecture relatively simple with fast convergence and steady-state performance, this adaptive filters are seen even today as an attractive option for a wide range of projects.

Many adaptive processing applications involve the reduction of noise, distortion, interference, echo, or any undesired signal [6, 32]. However, the degradation of this signal can vary with time and even be known initially. In this sense, the approach with an adaptive framework brings an interesting methodology to lead with this type of problem in several cases.

Adaptive systems work by changing the characteristics of their internal parameters. The current state is updated based on previous information which, through iterative processing, is automatically modified (adapted) to achieve a certain objective, depending on the case study and its engineering application.

Basically, a digital adaptive filter consists of two parts: a digital filter, that is usually a finite impulse response (FIR) or less commonly infinite impulse response (IIR) structures [33], which is responsible for the input signal processing, and an adaptive algorithm that upgrades and enhance the weights of this filter. We can define the input in time-discrete vector  $n$  as

$$\mathbf{x}(n) \equiv [x(n) \ x(n-1) \ \dots \ x(n-L+1)]^T, \quad (2-1)$$

in the same way, the vector of weights in time is given by

$$\mathbf{w}(n) \equiv [w_0(n) \ w_1(n) \ \dots \ w_{L-1}(n)]^T, \quad (2-2)$$

where  $T$  denotes the transpose operator. The output signal  $y(n)$  can be expressed by the following vectorial calculation

$$\begin{aligned} y(n) &= \mathbf{w}^T(n)\mathbf{x}(n) \\ &= \mathbf{x}^T(n)\mathbf{w}(n). \end{aligned} \quad (2-3)$$

The value of error  $e(n)$ , which measures the relationship between input noisy signal  $x(n)$  and the response referred to desired signal  $d(n)$ , whose difference is calculated by

$$\begin{aligned} e(n) &= d(n) - y(n) \\ &= d(n) - \mathbf{w}^T(n)\mathbf{x}(n). \end{aligned} \quad (2-4)$$

Figure 2.2 shows in a simplified form the basic structure of the adaptive filter utilized in ANC. In summary (vide Section 2.1.3 and 2.1.4), the objective is to recognize and attenuate the noise in  $x(n)$  comparing the filtered signal  $y(n)$  and the desired signal  $d(n)$  using the computation of the residual error  $e(n)$  which then will be used to improve the performance in the next filter iteration.

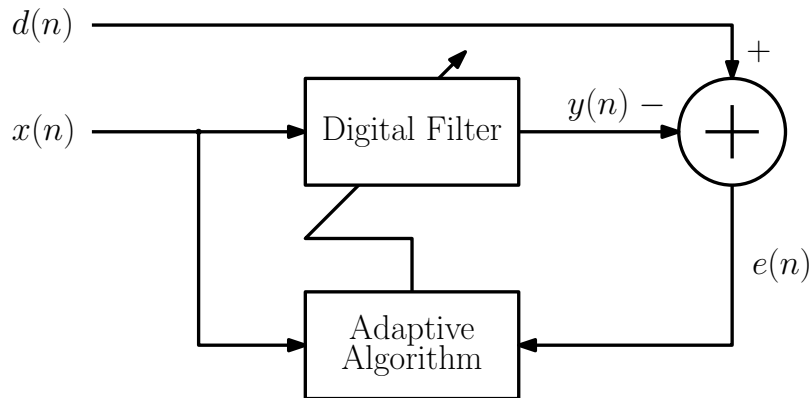


Figure 2.2: Block diagram of an Adaptive Filter.

It is important to mention that in this work the aim is to develop an adaptive algorithm applied in a transversal filter structure, or as it is more well known, an FIR structure in the feedforward topology for ANC. In the following sections, we present a conceptual review of the conventional ANC approach, using an FIR filter structure and the LMS algorithm.

### 2.1.1

#### MSE performance surface

The arrangement demonstrated in Figure 2.2, is used for the update of the digital filter coefficients, to optimize some performance parameters previously determined. The widest criteria applied to the evaluation of the system income is based on the *Mean Squared Error* (MSE) described by

$$J(n) = E[e^2(n)], \quad (2-5)$$

where  $E[\cdot]$  denotes the expected value operator.

In case of an FIR filter the value of  $J(n)$  depends of  $L$  weights  $w_0(n)$ ,  $w_1(n)$ , ...,  $w_{L-1}(n)$  of the Equation (2-2). If we consider the  $\mathbf{w}(n)$  as a sequence of deterministic values, then the value of the MSE function can be defined using (2-4), resulting in

$$J(n) = E[d^2(n)] - 2\mathbf{p}^T \mathbf{w}(n) + \mathbf{w}^T(n) \mathbf{R} \mathbf{w}(n), \quad (2-6)$$

where  $\mathbf{p}$  is the vector representing the cross-correlation between the desired and the input signals given by

$$\begin{aligned} \mathbf{p} &\equiv E[d(n)\mathbf{x}(n)] \\ &= [r_{dx}(0) \ r_{dx}(1) \ \dots \ r_{dx}(L-1)]^T, \end{aligned} \quad (2-7)$$

where

$$r_{dx}(k) \equiv E[d(n)x(n-k)], \quad (2-8)$$

and  $\mathbf{R}$  is the autocorrelation matrix of the input signal  $x$  given by

$$\begin{aligned} \mathbf{R} &\equiv E[\mathbf{x}(n)\mathbf{x}(n)^T] \\ &= \begin{bmatrix} r_{xx}(0) & r_{xx}(1) & \cdots & r_{xx}(L-1) \\ r_{xx}(1) & r_{xx}(0) & \cdots & r_{xx}(L-2) \\ \vdots & \cdots & \ddots & \vdots \\ r_{xx}(L-1) & r_{xx}(L-2) & \cdots & r_{xx}(0) \end{bmatrix}, \end{aligned} \quad (2-9)$$

where

$$r_{xx}(k) \equiv E[x(n)x(n-k)]. \quad (2-10)$$

Note that (2-6) is a general expression of the MSE function for an FIR causal filter with its coefficients  $\mathbf{w}(n)$ . Notice that the expression brings a quadratic function, in which each value of the filter coefficient returns an associated scalar value of MSE.

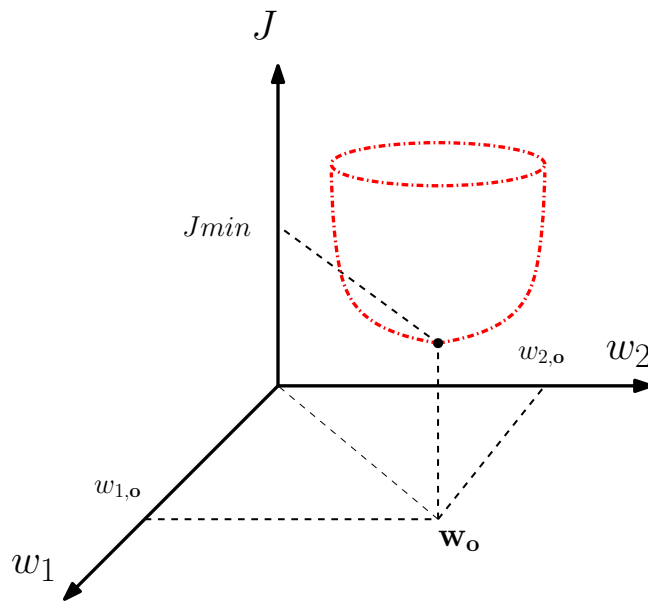


Figure 2.3: 3D MSE performance surface (case  $L = 2$ ).

For the case  $L = 2$ , we can observe in Figure 2.3 that the surface error returns a three-dimensional space where  $\mathbf{w}_o = [\mathbf{w}_{1,o} \ \mathbf{w}_{2,o}]^T$  is the value of the optimal coefficient vector and  $J_{min}$  is the MMSE.

The autocorrelation matrix defined in (2-9) performs a key role in the analysis and design of adaptive filters. Here, it is important to understand the

following properties [28]:

1. The autocorrelation matrix of the stationary stochastic process is symmetric. That is,  $\mathbf{R}^T = \mathbf{R}$ . Here we assume that real-valued for the function  $r_{xx}(k)$  and autocorrelation matrix.
2. The matrix  $\mathbf{R}$  of a stationary stochastic process is a Toeplitz matrix since all elements of any diagonal parallel to the main diagonal are equal.
3. All the eigenvalues of the autocorrelation matrix should be real since all its elements are symmetric and real. Therefore,  $\mathbf{R}$  is positive semidefinite (*i.e.* the eigenvalues are non-negative).

Finally, the optimal filter  $\mathbf{w}_o$  that minimizes the MSE of the objective function  $J(n)$ . Computing the derivative of the the MSE cost function in relation to the vector  $\mathbf{w}(n)$  of (2-6), we obtain

$$\mathbf{R}\mathbf{w}_o = \mathbf{p} , \quad (2-11)$$

which provides the solution to the adaptive filtering Wiener's problem (vide [6, 34]). To get the MMSE, we use the optimum weight vector  $\mathbf{w}_o$  of Equation (2-11) to  $\mathbf{w}(n)$  in (2-6), obtaining

$$J_{\min} = E[d^2(n)] - 2\mathbf{p}^T \mathbf{w}_o. \quad (2-12)$$

Combining the expressions of (2-6) and (2-11), we can obtain the mean square error as

$$\begin{aligned} J(n) &= J_{\min} + [\mathbf{w} - \mathbf{w}_o]^T \mathbf{R} [\mathbf{w} - \mathbf{w}_o] \\ &= J_{\min} + \boldsymbol{\varepsilon}(n)^T \mathbf{R} \boldsymbol{\varepsilon}(n) , \end{aligned} \quad (2-13)$$

where

$$\boldsymbol{\varepsilon}(n) \equiv \mathbf{w}(n) - \mathbf{w}_o \quad (2-14)$$

is the weight misalignment vector, is nothing more than the difference between the filter coefficients and the optimal solution.

### 2.1.2 Steepest Descent method

As shown in Figure 2.3, the expression of the MSE Equation (2-13) is a quadratic function of weights that can be depicted as a positive concave hyperbolic surface. Newton Methods [10] has fast convergence, but the estimate of  $\mathbf{R}^{-1}$  involves a certain heavy computational requirement.

Due to the context previously described, the steepest descent method is an iterative technique ideally appropriate to derive the adaptive algorithm, since the surface error can guarantee the definition of the function as quadratic concerning the filter values  $w_l$ . For that reason, the method of steepest descent is widely used in linear programming and optimization problems. The concept of the steepest descent can be implemented in the form as follows:

$$\mathbf{w}(n+1) = \mathbf{w}(n) - \frac{\mu}{2} \nabla J(n), \quad (2-15)$$

which  $\mu$  is called convergence factor or, as more known, *step size*. This variable controls the stability and the degree of decay in the minimized surface (or in other words, the learning curve). The term  $\nabla J(n)$  denotes the gradient of the error related to  $\mathbf{w}(n)$ . In Equation (2-6), we can easily calculate the error gradient

$$\nabla J(n) = -2\mathbf{p}(n) + 2\mathbf{R}\mathbf{w}(n). \quad (2-16)$$

Substituting (2-16) in (2-15), we have the final expression of steepest descent algorithm, given by

$$\mathbf{w}(n+1) = \mathbf{w}(n) + \mu[\mathbf{p} - \mathbf{R}\mathbf{w}(n)]. \quad (2-17)$$

Note that, when  $\mathbf{w}(n)$  converges to  $\mathbf{w}_o$ , the minimal point of the performance surface is reached, *i.e.*,  $\nabla J(n) = 0$ .

### 2.1.3 LMS algorithm

In Equation (2-17) we can see that the incremental value from the previous stage of filter vector  $\mathbf{w}(n)$  to  $\mathbf{w}(n + 1)$  is in the negative direction of the gradient. Then, the weight tracking will follow approximately in the way of the steepest descent method in the performance surface evaluated. However, in many practical applications, the values of the signals  $d(n)$  and  $x(n)$  are unknown.

Widrow *et al* [10] proposed the fundamental idea to use of the instantaneous value of the error ( $\hat{J}(n) = e^2(n)$ ) to estimate the MSE in (2-5). Thus, the gradient estimate value using LMS algorithm is simplified to the instantaneous gradient of an unique squared error sample

$$\nabla \hat{J}(n) = 2e(n)[\nabla e(n)], \quad (2-18)$$

where from the expression (2-4), we have that the gradient of the residual error is

$$\nabla e(n) = -\mathbf{x}(n). \quad (2-19)$$

Then, the gradient of the estimated function returns

$$\nabla \hat{J}(n) = -2\mathbf{x}(n)e(n). \quad (2-20)$$

Substituting the computed derivative result of (2-20) into the steepest descent Equation (2-17), we obtain the formulation of the update Equation that can be defined as:

$$\mathbf{w}(n + 1) = \mathbf{w}(n) + \mu\mathbf{x}(n)e(n). \quad (2-21)$$

Equation (2-21) describes the well-known LMS algorithm or stochastic gradient algorithm. This method is relatively simple and does not require squaring, averaging, or differentiating [28]. Beyond this, it is possible to observe that the gradient estimate is unbiased and the expected value of the weight

vector converges to the Wiener filter solution (Equation (2-11)).

Figure 2.4 shows a generic block diagram and the Widrow-Hopf algorithm to FIR filters [10], which is summarized in Table 2.1 as follows.

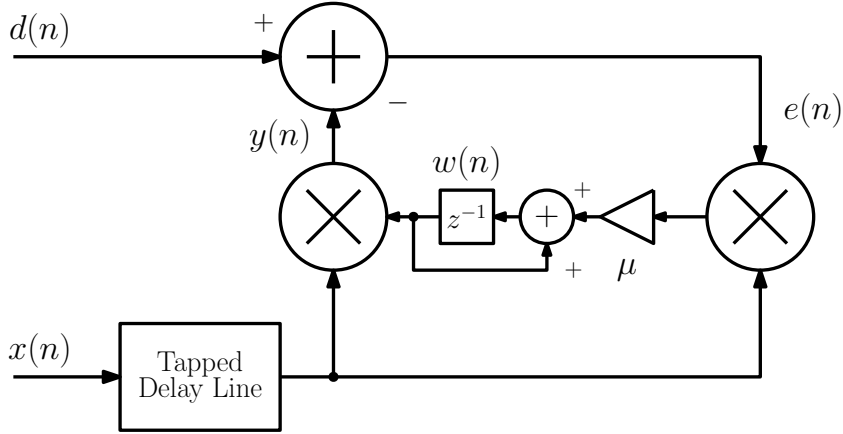


Figure 2.4: Block diagram of an LMS adaptive filter framework.

Table 2.1: Steps to deploy the LMS algorithm.

Step	Equation
1) Choose the parameters and initial conditions: the filter order, the step size and the initial weight vector value (time $n = 0$ ).	$L > 0 \in \mathbb{Z}; 0 < \mu < 1$ and $\mathbf{w}(0)$
2) Compute the adaptive filter output	$y(n) = \sum_{l=0}^{L-1} w_l(n)x(n-l)$
3) Compute the signal of residual error	$e(n) = d(n) - y(n)$
4) Update the weight vector, applying the gradient and using LMS	$w_l(n+1) = w_l(n) + \mu x(n-l)e(n)$

In terms of computational complexity, the Equation of step 2 requires  $L$  multiplications and  $L - 1$  additions. To coefficient update in step 4 are need  $L + 1$  multiplications and  $L$  additions. The following section presents another fundamental concept to the research of this work.

However, as cited previously, to deal with the special noise cancelling conditions, a complementary framework is added to the LMS algorithm to enhance the performance of ANC systems. In Section 2.1.4 this approach is described in detail and derived.

### 2.1.4

#### Base Model: FXLMS

In this section, we present the general and main structure used to deploy any algorithm applied to ANC. In particular, we consider as basic example the framework for the well-known *filtered-X Least Mean Square* algorithm.

This approach unifies the network which brings the filtered secondary path response with the adaptive algorithm described in 2.1.3. The first one aims to minimize the influence of the transfer function of the primary path (*i.e.* the way that the noise is transmitted) in the final calculation of the residual error associated with the suppression of the noise signal.

In the following steps, this approach is presented in detail. Briefly, the basic structure of the filtered-X LMS (FXLMS) algorithm can be described by

$$e(n) = d(n) - [\mathbf{x}^T(n)\mathbf{w}(n)] * s(n) + v(n), \quad (2-22)$$

where

$$\begin{aligned} \mathbf{v}(n) &= [v(0) \ v(n-1) \ \dots \ v(L-1)] \quad \text{and} \\ \mathbf{s}(n) &= [s_0(n) \ s_1(n) \ \dots \ s_{L-1}(n)]^T. \end{aligned} \quad (2-23)$$

To minimize the MSE, the algorithm updates  $\mathbf{w}(n)$  towards the negative value of the gradient of  $J(n)$  using the step size  $\mu$  according to

$$\mathbf{w}(n+1) = \mathbf{w}(n) - \frac{\mu}{2} \nabla \hat{J}(n). \quad (2-24)$$

We have from the Section 2.1.3 that  $\nabla \hat{J}(n) = 2[\nabla e(n)]e(n)$  is the instantaneous estimate of the gradient of the MSE cost function given by

$$\begin{aligned} \nabla e(n) &= -x(n) * s(n) \\ &= -x'(n), \end{aligned} \quad (2-25)$$

where  $s(n)$  is the  $n$ th component of the estimation of  $\mathbf{s}(n)$ . This derivative response is the filtered-X input. After mathematical arranging of the terms, it is possible to obtain the general equation of the FXLMS given by

$$\mathbf{w}(n+1) = \mathbf{w}(n) + \mu \mathbf{x}'(n)e(n). \quad (2-26)$$

Therefore, summarizing the step described in about the fundamentals of adaptive processing systems in Section 2.1 and the LMS algorithm in Section 2.1.3, we can define in Algorithm 1 the main steps of the FXLMS algorithm.

---

**Algorithm 1** FXLMS Algorithm

---

**Require:**  $\mathbf{x}(n) = [x(n) \ \dots \ x(n - L + 1)]^T$ ,  $\mathbf{w}(n) = [w_0(n) \ \dots \ w_{L-1}(n)]^T$

**Require:**  $d(n), P(z), S(z)$

**Require:**  $\mu$

**while**  $n \leq L$  **do**

$$y(n) = \mathbf{x}(n)^T \mathbf{w}(n)$$

$$e(n) = d(n) - \mathbf{s}(n) * (\mathbf{w}(n)^T \mathbf{x}(n))$$

$$\mathbf{w}(n + 1) = \mathbf{w}(n) + \mu e(n) \mathbf{x}'(n)$$

**end while**

---

As described before in the beginning of Chapter 2, Figure 2.5 illustrates as well the two main approaches in the ANC field, namely, the feedforward and feedback structures.

Basically, the active noise cancellation system originates from a dynamic architecture that is designed to compute a determined signal considered “noise” through the secondary path where the same amplitude and inverse-phased signal will be transmitted. The expected result of this operation is the sound destructive interaction that causes the cancellation or hard reduction of the spurious signal in the system output.

For some problem of noise cancellation that the system and/or the signals are nonlinear (i.e. *Nonlinear Active Noise Cancellation*, NLANC), Figure 2.6 depicts a different framework by adding a module of expansion seeking to reach the nature of the input of this specific case is applied.

Starting from these classic models, a wide field of research in ANC and its applications was growing developing a series of novel algorithms and networks for solving a variety of problems using active cancellation systems in different areas of science and engineering, which confirmed its efficiency, versatility, adaptation capacity, and technological advance.

Although the FXLMS came to realize an adaptive ANC system able to lead with the white noise cancelling, as cited in Section 1, in the dynamic

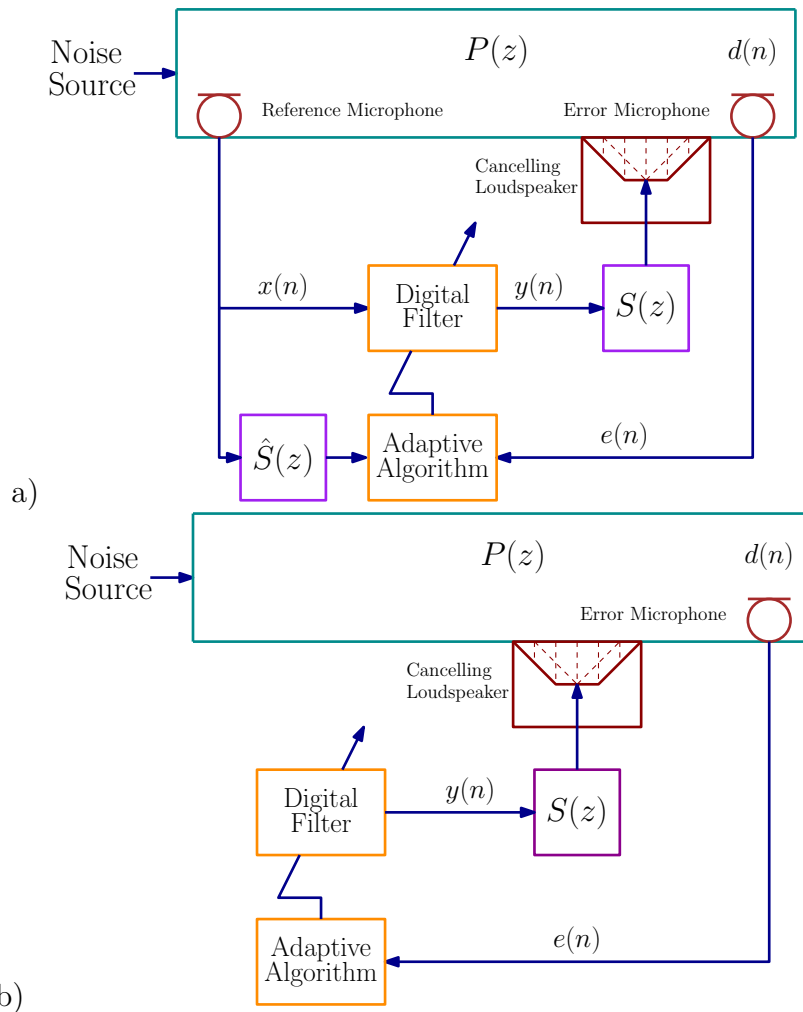


Figure 2.5: Diagram of FXLMS frameworks: (a) feedforward; (b) feedback.

system with non-linearities or non-average statistical signals the performance of the filtered-X LMS is completely wasted. For this reason, some methodology that takes into account the stochastic characteristics of the signal must be adopted, thus making the treatment of the physical features of this signals and its systems involved feasible [12].

Some combinations and improvements, in the context of the most relevant and recent innovations, are presented with more details in the Section 2.2.

## 2.2 Robust Filtering Methods

Throughout the years, and still more specifically in the recent context, the importance and growing demand of related research beyond the success of

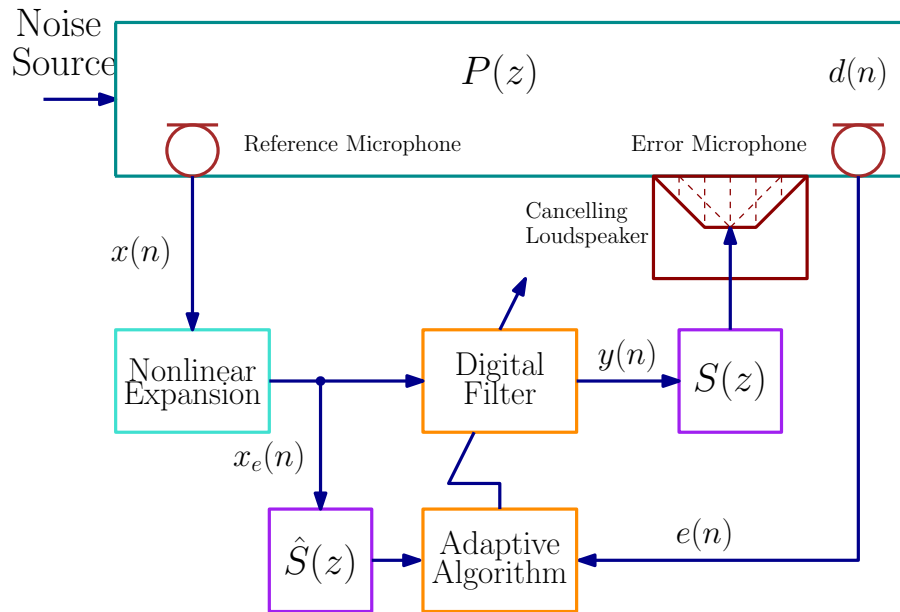


Figure 2.6: Diagram of the feedforward FXLMS NLANC model.

some approaches widely studied turned the field of ANC into a high and broad area of knowledge.

Some surveys around the most consolidated and promising ANC methods, frameworks, and algorithms have been carried out. The works realized by a group of researchers and engineers in the area of signal processing [12] mapped the brief history of this application and pointed out the state-of-the-art in the last decade related to linear ANC and non-linear ANC (NLANC) [13].

Several ANC techniques have been discussed along the years with their research impact [12, 13]. Here, we discuss in what follows some of the most efficient applied approaches to ANR and their perspectives about the range of different frameworks like: the filtered-X (*vide* Section 2.1.4) [35] and its novel analogies such as filtered-S [36], and others more advanced as Lattice, Subband [25, 37], Affine Projection (AP) [21, 38], and others.

Among the adaptive algorithms are the classical LMS and unfolding methods such as Log, Least-Mean  $p$ -power (LMP) [16], fast RLS [15], and Kalman filter and its variants [39]; the Heuristic methods: Genetic algorithm or Particle swarm [17] between others. Another trend is exploiting the diverse optimization techniques with a given objective function that include gradient

(steepest descent, SG,  $q$ -version [40]), Newton (and other combinations like Newton-Raphson or *quasi*-Newton) techniques.

We still have some approaches in the literature studying the different uses in auxiliary techniques such as variable step-size (VSS) [14], noise model  $\alpha$  – *stable* [41], and other ANC models like psychoacoustics system, sparse techniques, convex combination of algorithms, fractional order approaches, and robust algorithms against non Gaussian noise [42].

Lastly, another approach has considered the study and development of novel objective functions used to develop robust algorithms using methods like the correntropy criterion [21], hyperbolic trigonometric functions [22] and an exponential conjugated version [24], the M-estimator method [25] and many others. This point of view is the main idea to be exploited in the development of the proposed algorithm of this research.

In Section 2.3 we present some important analytical concepts related to the convergence analysis that adaptive algorithms applied in ANC should consider.

### 2.3 Statistical Analysis

This section summarizes the stochastic analysis of an adaptive algorithm applied to noise cancellation. To expose that, we choose to explain using the concepts using the LMS and filtered-X structure or in other words, the most applicable framework in the ANC known as FXLMS.

The aim is to employ a statistical approach to study the behavior of the FXLMS in terms of its learning performance. Here, this can be interpreted like a more advanced extension from Section 2.1.

When evaluating the convergence of an adaptive algorithm, some assumptions and observations should be inserted or tested in the mathematical development of equations to guarantee that the filter does not take severe risks in terms of its stability and causality [43].

### 2.3.1 Steady-State Solutions

For the definition of minimal conditions of convergence in adaptive algorithms, two assumptions are made:

1.  $x(n)$  e  $v(n)$  are (wide sense) stationary stochastic processes with zero mean (*i.e.*,  $E[x(n)] = 0$  and  $E[v(n)] = 0$ );
2.  $w(n)$  is statistically independent of  $x(n)$ . This condition is already met simply when the step-size  $\mu$  has a very low value.

Based on this previous hypothesis and the equation of the residual error estimation to FXLMS, we can present a solution to the Wiener problem of assumption 1 as

$$\begin{aligned}
 E[e^2(n)] &= \sigma_d^2 + \sigma_v^2 \\
 &+ 2 \sum_{i=0}^{L-1} s_i E[\mathbf{x}^T(n-i)d(n)] \mathbf{w} \\
 &+ \mathbf{w}^T \sum_{i=0}^{L-1} \sum_{j=0}^{L-1} s_i s_j E[\mathbf{x}^T(n-i)\mathbf{x}(n-j)] \mathbf{w}.
 \end{aligned} \tag{2-27}$$

Minimizing the Equation (2-27) and adding the condition of steady state in order to obtain a formulation that complies with the hypothesis that the algorithm will reach a Wiener's solution (see more details in Section 2.1.1):

$$\mathbf{w}(\infty) = -\mathbf{R}_{\text{ss}}^{-1} \mathbf{p}_s, \tag{2-28}$$

where

$$\mathbf{R}_{\text{ss}}^{-1} = E[\hat{\mathbf{X}}(n)\hat{\mathbf{s}}\mathbf{s}^T\mathbf{X}^T(n)] = \sum_{i=0}^{L-1} \sum_{j=0}^{L-1} s_i \hat{s}_j \mathbf{R}_{i-j}, \tag{2-29}$$

$$\mathbf{p}_s = E[d(n)\hat{\mathbf{X}}(n)\hat{\mathbf{s}}] = \sum_{i=0}^{L-1} \hat{s}_i E[\mathbf{x}(n-i)d(n)]. \tag{2-30}$$

that  $\hat{\mathbf{s}}$  represents the estimation of its secondary path in the referred FXLMS model.

In summary, the FXLMS algorithm converges to the Wiener solution when the secondary path (Figure 2.5) is exactly estimated. Meanwhile, we have as a consequence a deterioration in the algorithm performance in noise cancellation. To treat this question, an imperfect secondary path is utilized in the study.

### 2.3.2 Parametric Convergence Analysis

In what follows, the concept of the steady state described above is applied to reach a convergence state of the fundamental parameters of the adaptive filtering algorithm.

#### 2.3.2.1 Mean Behavior of the Weight Vector

Analogously to Equation (2-14), to determine the difference between the weight vector and required steady-state value, we have:

$$\tilde{\mathbf{w}}(n) = \mathbf{w}(n) - \mathbf{w}(\infty), \quad (2-31)$$

Subtracting  $\mathbf{w}(\infty)$  in both sides of the FXLMS filter equation, we obtain

$$\tilde{\mathbf{w}}(n+1) = \tilde{\mathbf{w}}(n) - \mu \mathbf{G}(n) \tilde{\mathbf{W}}(n) - \mu \mathbf{b}(n), \quad (2-32)$$

where

$$\mathbf{G}(n) = \hat{\mathbf{X}}(n) \hat{\mathbf{s}} \mathbf{X}_s^T(n), \quad (2-33)$$

and

$$\begin{aligned} \mathbf{b}(n) &= \hat{\mathbf{X}}(n) \hat{\mathbf{s}}(d(n) + v(n) + \mathbf{X}_s^T(n) \mathbf{W}(\infty)) \\ &= \hat{\mathbf{X}}(n) \hat{\mathbf{s}}(d(n) + v(n) + \mathbf{s}^T \mathbf{X}^T(n) \mathbf{w}(\infty)). \end{aligned} \quad (2-34)$$

are the expression of the autocorrelation (2-29) and cross correlation (2-30) of the input signal  $\mathbf{X}(n)$  and the primary path response  $d(n)$ .

### 2.3.2.2 MSE Behavior

In this section, we deepen the mathematical development initiated in 2.1.1. Applying to the base model the concept of steady state, which the concern is about the convergence of the evolution of the learning curve in the MSE of the least squares error model (where the objective function  $J(n) = E[e(n)^2]$ ).

Aiming to achieve this condition in the model, we first use a novel formulation of the residual error signal proposed using the term of the weight vector in a state of stationary condition.

$$e(n) = d(n) + v(n) + \mathbf{X}_s^T(n)(\mathbf{W}(n) + \mathbf{W}(\infty)). \quad (2-35)$$

where

$$\begin{aligned} \mathbf{X}_s^T(n) &= \mathbf{s}(n)\mathbf{X}^T(n) \\ &= \begin{bmatrix} s_0(n)\mathbf{x}(n) \\ s_1(n)\mathbf{x}(n-1) \\ \vdots \\ s_{L-1}(n)\mathbf{x}(n-L+1) \end{bmatrix}, \end{aligned} \quad (2-36)$$

is the input vector weighted by coefficients of the secondary path, and

$$\mathbf{W}(n) = \begin{bmatrix} \mathbf{w}(n) \\ \mathbf{w}(n-1) \\ \vdots \\ \mathbf{w}(n-L+1) \end{bmatrix}, \quad (2-37)$$

is the augmented weight vector. With this, the expression of the MSE is given by

$$\begin{aligned} J(n) &= E[e(n)^2] \\ &= E\left[\left(d(n) + v(n) + \mathbf{X}_s^T(n)(\mathbf{W}(n) + \mathbf{W}(\infty))\right)^2\right], \end{aligned} \quad (2-38)$$

which can be expressed in terms of the variances  $\sigma_d^2$ ,  $\sigma_v^2$  (as in Equation (2-27))

and all the estimates related to the matrix  $\mathbf{X}_s^T(n)$ , the augmented vector  $\mathbf{W}(n)$ , and its steady-state version  $\mathbf{W}(\infty)$ .

### 2.3.2.3 Steady-State Condition

The steady state of the FXLMS model can be expressed by

$$J(\infty) = J_{\min} + J_{ex}, \quad (2-39)$$

where

$$\begin{aligned} J_{\min} &= \sigma_d^2 + \sigma_v^2 \\ &+ 2E \left[ d(n)\mathbf{X}_s^T(n) \right] \mathbf{W}(\infty) \\ &+ \text{tr} \left( E \left[ \mathbf{X}_s(n)\mathbf{X}_s^T(n) \right] E \left[ \mathbf{W}(\infty)\mathbf{W}^T(\infty) \right] \right), \end{aligned} \quad (2-40)$$

is the minimum MSE that the FXLMS algorithm can achieve given the Wiener solution, and

$$J_{ex} = \text{tr} \left( E \left[ \mathbf{X}_s(n)\mathbf{X}_s^T(n) \right] \text{vec}^{-1}(\delta(\infty)) \right), \quad (2-41)$$

which  $\text{vec}^{-1}(\delta(\infty))$  is the inverse of impulse response of the weight vector in steady-state. In resume, the Equation 2-41 is the excess MSE (EMSE) which is introduced because of the fluctuations of the adaptive coefficients.

It is important to note that the computational complexity and ways of simplifying the system should still be studied. Moreover, comparative tests with respect to different methodologies, techniques, and models approached in each study case should also be performed.

In Section 2.2 we presented some methods investigated from the different recent literature, seen actually as a scientific reference in the literature of the area focused on high robustness of adaptive filtering.

## 2.4 Summary

This chapter discussed the theoretical fundamentals of active noise cancellation techniques. To this end, we reviewed the concepts of adaptive signal processing, the general ideas associated with the noise cancellation methods, an example using the well-known LMS algorithm and the filtered-X framework, with the statistical analysis that includes the stability and the steady-state behaviour as referred to in the literature.

### 3

## Hyperbolic Exponential Kernel M-estimate Algorithm

In this chapter, we derive the proposed FXHEKM ANC algorithm, and carry out its stability, the steady state and the computational complexity analyses. In the following sections, the model adopted in this work considers a method for robust adaptive processing in an ANC system.

### 3.1

#### System modeling

Consider a classical noise cancellation problem, where we try to suppress the noise contaminating the environment [8]. This task is performed by an adaptive ANC system, as shown in Figure 3.1.

The discrete-time signal  $x(n)$  describes the input signal;  $y(n)$  represents the output signal;  $e(n)$  is the residual error of the system in the procedure for computing the value the error to update the adaptive algorithm, *i.e.* in case of the purposed algorithm based on the *Hyperbolic tangent Exponential generalized Kernel M-estimate* (HEKM) function, which will be demonstrated in detail in Section 3.2.

The calculation of these variables is described in detail in the following section. Note that in this system, the input signal is used directly in the error estimation and the calculation of the filter response.

Basically, the model components crossed by a dashed line can be defined as an adaptive filter, consisting of: *i*) a digital filter (here we consider an FIR structure) to develop the signal processing and *ii*) the adaptive algorithm that realizes the weight update of this filter.

The signal related to the estimation of input noise  $x(n)$  of the filtered output can be expressed by the vector operation

$$y(n) = \mathbf{w}(n)^T \mathbf{x}(n), \quad (3-1)$$

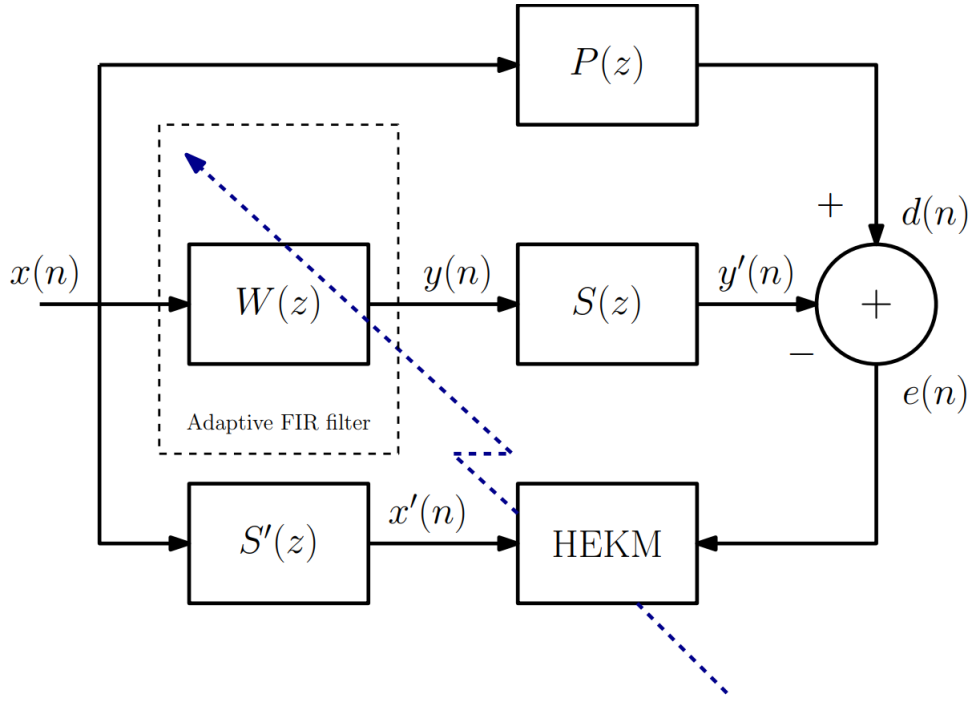


Figure 3.1: Block diagram of the proposed Adaptive Noise Cancellation system.

Then, the value of the residual error in the system to be computed is defined as the difference between the desired signal and the filtered output, expressed by

$$\begin{aligned}
 e(n) &= d(n) - y'(n) \\
 &= p(n) * x(n) + v(n) - s(n) * (\mathbf{w}(n)^T \mathbf{x}(n)) \\
 &= d(n) - \mathbf{w}(n)^T \mathbf{x}'(n),
 \end{aligned} \tag{3-2}$$

where  $d(n)$  is the desired signal and  $y'(n)$  is the noisy input estimation computed by the adaptive filter. The signal  $v(n)$  is the noise of the measurement error, and the response of  $p(n)$  and  $s(n)$  is the respective impulse response of primary  $P(z)$  and secondary path  $S(z)$  at time  $n$  and  $*$  denotes the operation of linear convolution. The  $\mathbf{x}'(n)$  is the well-known *filtered-X* signal, computed from the input of the system by the  $S'(n)$  (or the second path estimation), employed to compute the model response.

## 3.2

### Derivation of the Proposed FXHEKM Algorithm

Initially, we define the objective function of the method HEKM, which is robust against non-Gaussian noise. This work aims to find a robust function that can obtain a satisfactory relation between fast convergence and the lowest MSE level, both for Gaussian and impulsive signals. To obtain the formulation of the method, two steps are needed:

1. Derivation of the objective function of the adaptive filter algorithm, and
2. Insert 1 inside the update equation of the ANC model (filtered-X structure).

After some theoretical study and an experimental procedure for performance evaluation, the proposed approach consists of adopting an objective function based on the hyperbolic tangent of a kernel of the residual error computation (Equation (3-2)), which can be defined by

$$J\{\mathbf{w}(n)\} = - \sum_{k=1}^N \rho^{N-k} \frac{1}{\alpha} \tanh \left( \alpha \exp^{-\eta|e(n)|^p} \right), \quad (3-3)$$

where  $\alpha > 0$  is a mathematically convenient variable with constant value and  $\eta, p > 0$  are constants to set the exponential behavior of the kernel and  $\rho$  is an exponential value variable known as *forgetting factor* with length  $N$ .

Therefore, we can observe the geometrical aspects explained in Section 2.1.1 for the LMS algorithm, which is now used for the FXHEKM algorithm. Here, we have three different parameters which can set the behavior of the proposed objective function. The fundamental mission here is to put better parameters in the algorithm adaptive equation, aiming to find the value that minimizes optimally the value of  $\mathbf{w}(n)$ .

In the sequence, the graphs below show this phenomenon and its *trade-of* issues. Firstly, in Figure 3.2, we have an objective function curve plotted related to the  $e(n)$  (because the  $J(n)$  is a function of the weight vector and

the residual error) observe how this curve can be more deeply and sharp as the value of  $\alpha$  increases.

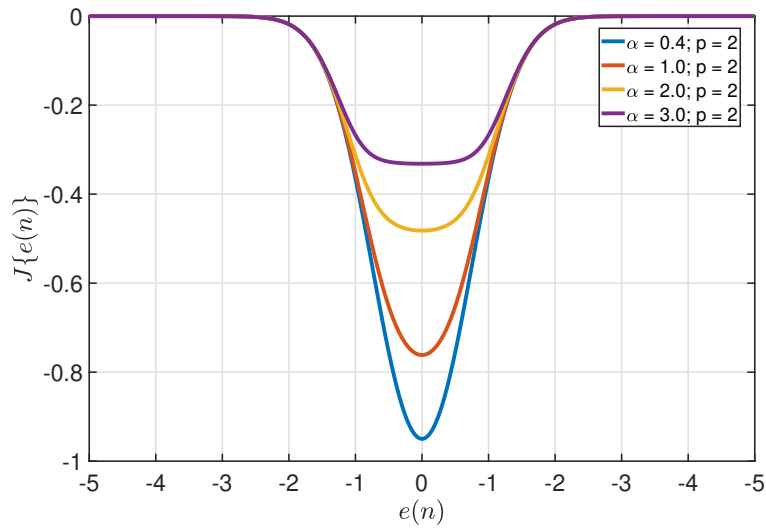


Figure 3.2: Objective function of HEKM related to the parameter  $\alpha$ .

In the other scenario, using the fixed values of  $\alpha$  and  $\eta$ , when we change the parameter  $p$ . Figure 3.3 represents a range of possible curves, from an envelope with an extremely sharp peak to a plateau around the minimum value.

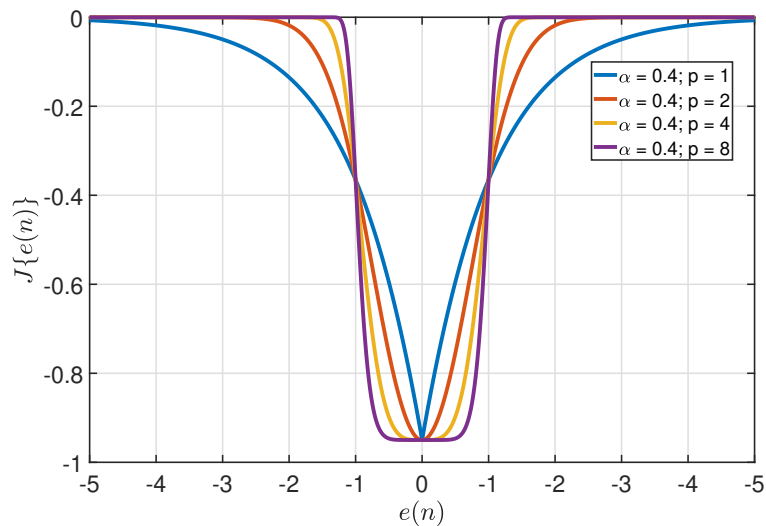


Figure 3.3: Objective function of HEKM related to the parameter  $p$ .

Finally, the value of the  $\eta$  is tested maintaining the other, seeking to

evaluate the range of options to insert in the FXHEKM in the following simulations of the study case.

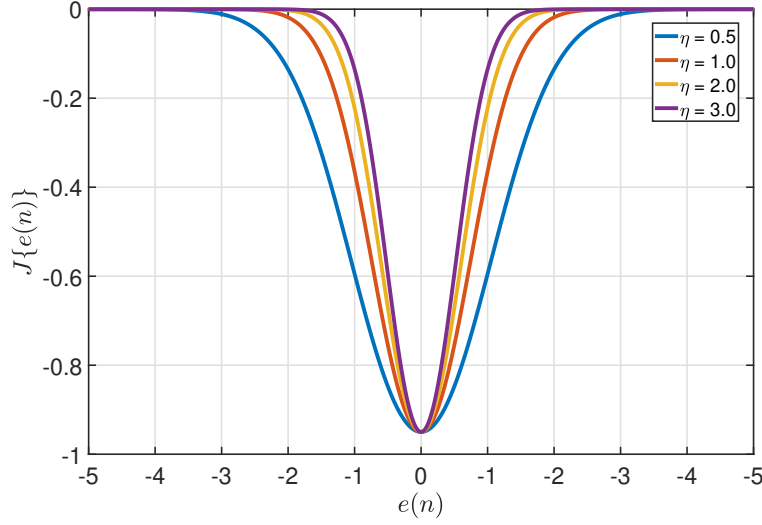


Figure 3.4: Objective function of HEKM related to the parameter  $\eta$ .

For the last parameter, the variation between the curves in the shape of the inverted bell is a little less sensitive, but we observe a kind of narrowing when you increase the value of  $\eta$ .

Afterward, the derivative of the objective function is computed by the gradient descent (GD) method [44], we get the expression for the term of the update,

$$\begin{aligned}
 \frac{\partial J\{\mathbf{w}(n)\}}{\partial \mathbf{w}(n)} &= -\frac{1}{\alpha} \sum_{k=1}^N \rho^{N-k} \frac{\partial \{\tanh(\alpha \exp^{-\eta|e(n)|^p})\}}{\partial \mathbf{w}(n)} \\
 &= -\frac{1}{\alpha} \sum_{k=1}^N \rho^{N-k} \operatorname{sech}^2(\alpha \exp^{-\eta|e(n)|^p}) \frac{\partial \{\alpha \exp^{-\eta|e(n)|^p}\}}{\partial \mathbf{w}(n)} \\
 &= -\frac{1}{\alpha} \sum_{k=1}^N \rho^{N-k} \operatorname{sech}^2(\alpha \exp^{-\eta|e(n)|^p}) \alpha \exp^{-\eta|e(n)|^p} \frac{\partial \{-\eta|e(n)|^p\}}{\partial \mathbf{w}(n)} \\
 &= -\sum_{k=1}^N \rho^{N-k} \operatorname{sech}^2(\alpha \exp^{-\eta|e(n)|^p}) \exp^{-\eta|e(n)|^p} \\
 &\quad (-\eta)p|e(n)|^{p-1} \operatorname{sign}(e(n)) \frac{\partial \{e(n)\}}{\partial \mathbf{w}(n)},
 \end{aligned}$$

and taking the derivative of Equation (3-2) we have  $\partial e(n)/\partial \mathbf{w}(n) = -\mathbf{x}'(n)$ ,

then we can obtain the formalized expression of the gradient terms given by

$$\begin{aligned} \frac{\partial J\{\mathbf{w}(n)\}}{\partial \mathbf{w}(n)} = & \\ & - \eta p \sum_{k=1}^N \rho^{N-k} \operatorname{sech}^2 \left( \alpha \exp^{-\eta|e(n)|^p} \right) \exp^{-\eta|e(n)|^p} |e(n)|^{p-1} \operatorname{sign}(e(n)) \mathbf{x}'(n), \end{aligned} \quad (3-4)$$

where

$$\mathbf{x}'(n) = s'(n) * \mathbf{x}(n), \quad (3-5)$$

represent the filtered version of input vector  $\mathbf{x}(n)$  convoluted by response of the secondary path estimation of  $S'(z)$  in the ANC system. Therefore, the expression of this derivation generates the *filtered-X Hyperbolic Tangent Generalized Kernel M-estimate* (FXHEKM) model.

Note that, analogously to the objective function of the proposed algorithm, the derivative expression of Equation (3-4) is so sensitive to a certain number of parameters. Figure 3.5 shows the curves related to the parameter  $\alpha$  of the objective function of the HEKM method.

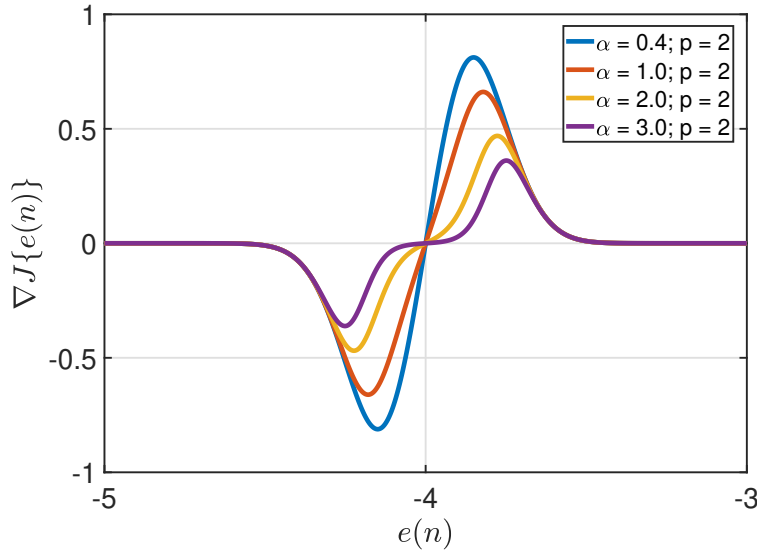


Figure 3.5: Derivative of objective function get the FXHEKM related to the set of parameter  $\alpha$ .

The change of this variable can generate some differentiations in the curve

behavior. Note that here, in the derivative forms, we have an envelope with an inflection point, and then a species of nonlinearity generated by the gradient. For the case of  $\alpha$ , a shift and reduction of the the peak value happen when the value of the parameter increases. Next, Figure 3.7 shows the comparison between the curves when we set different values of the  $p$ .

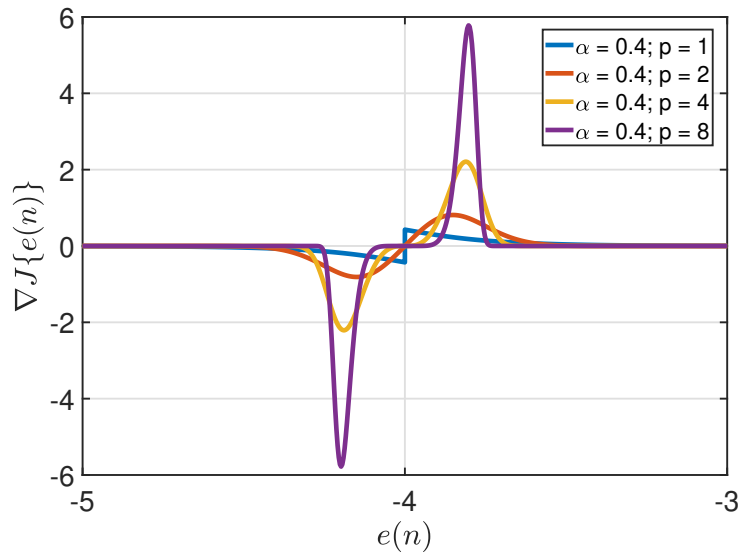


Figure 3.6: Derivative of objective function get the FXHEKM related to the set of parameter  $p$ .

This scenario can be the most sensitive trade-off in the whole analysis realized in this study. The behavior of the curves changes the type, height, width, and distance between the peaks around the inflection point of the curve. Here, it is an important point to carry out to choose the value of the adaptive equation. If we repair in the high value of  $p$  like 3.0, we get an impulsive peak curve in the adaptive equation and it would be unstable for the algorithm.

Lastly, the Figure 3.6 brings the evaluation of the derivative curves of  $\nabla J(\mathbf{w}(n))$ . Here, we can conclude that the smallest value of this parameter results in an almost linear curve while the highest value can return a huge peak around the inflection point. The following analyses set the best range for the parameter as  $\eta \approx [1.0, 2.0]$ . For the simulations described in Section 3.4.2, the values considered in the standard version of FXHEKM defined to simulations

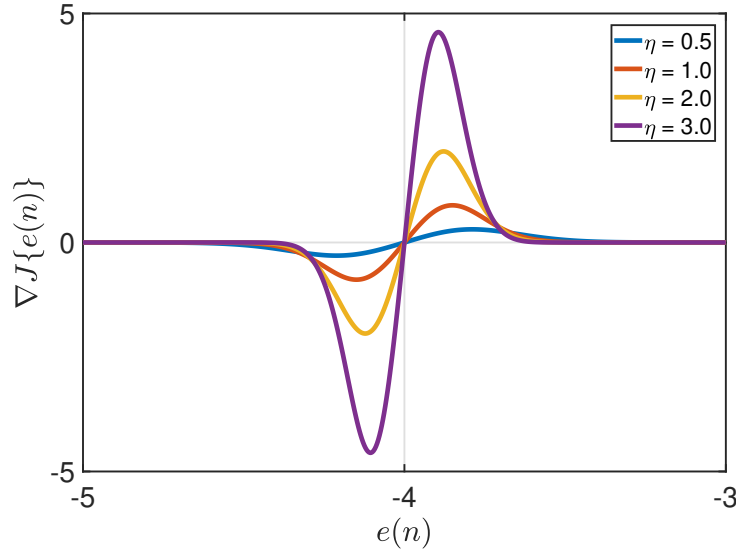


Figure 3.7: Derivative of objective function get the FXHEKM related to the set of parameter  $\eta$ .

of this work are:  $\alpha = 1.0$ ,  $\eta = 1.0$  and  $p = 2.0$ .

Therefore, let us consider the definition for the update state of the weight vector  $\mathbf{w}(n)$ , defined in the adaptive filter theory Section 2.1 [6], realized by the adaptive processing of the algorithm for the proposed model that can be computed as

$$\begin{aligned}
 \mathbf{w}(n+1) &= \mathbf{w}(n) - \Delta \mathbf{w}(n) \\
 &= \mathbf{w}(n) - \frac{\partial J\{\mathbf{w}(n)\}}{\partial \mathbf{w}(n)} \\
 &= \mathbf{w}(n) + \mu \sum_{k=1}^N \rho^{N-k} \text{sech}^2 \left( \alpha \exp^{-\eta|e(n)|^p} \right) \\
 &\quad \exp^{-\eta|e(n)|^p} |e(n)|^{p-1} \text{sign}(e(n)) \frac{\mathbf{x}'(n)}{\delta + \|\mathbf{x}'(n)\|_2^2} \\
 &= \mathbf{w}(n) + \mu \sum_{k=1}^N \rho^{N-k} \phi(e(n)) |e(n)|^{p-1} \mathbf{x}'(n),
 \end{aligned} \tag{3-6}$$

where  $\mu = \eta p$  represents the value of the step-size and the generalized expression

$$\phi(e(n)) = q(e(n)) \text{sech}^2 \left( \alpha \exp^{-\eta|e(n)|^p} \right) \exp^{-\eta|e(n)|^p} \frac{\text{sign}(e(n))}{\delta + \|\mathbf{x}'(n)\|_2^2}, \tag{3-7}$$

which  $\|\mathbf{x}'(n)\|_2^2 > 0$  is a  $l^2$ -norm of the input vector used for the final improved normalized version. As a result, an extremely small positive value  $\delta$  is increased as a regularization factor to avoid a division by zero.

Lastly, to obtain a reliable response concerning the learning curve variations, we introduce a robust strategy against non-Gaussian noises (*i.e.* impulsive) as a combined tool in the full proposed model by employing the function  $q(e(n))$  based on the  $M$ -estimator method, see the work of Yu *et al* [42], given by

$$q(e(n)) = \begin{cases} 1, & |e(n)| < \zeta \\ 0, & |e(n)| \geq \zeta \end{cases}, \quad (3-8)$$

where  $\zeta$  is the threshold coefficient of the  $M$ -estimate method that controls the response of this function in the update term in (3-6), based on the comparison with the modulus of the residual error.

This function applies a kind of “penalty” factor occurring in the maintenance or null of the new value of  $\Delta\mathbf{w}(n)$  in the adaptive filter update equation. With this, the algorithm decides to consider (or not) in the current stage, the same previous value or the improved learned new one. Then, it turns the model to be able to lead quickly with the fast non-linear variations related to the impulsive signals.

As can be seen in what follows, in Algorithm 2 the proposed FXHEKM algorithm is described and listed step-by-step in detail.

### 3.3 Statistical Analysis

This section describes a statistical analysis of the FXHEKM algorithm. In particular, we consider the stability conditions for the proposed algorithm. This part of the study aims to ensure the basis that provides mathematical guarantees to the proposed approach as evidenced in the literature [43]. In particular, we analyze the stability conditions and derive formulas to predict

---

**Algorithm 2** FXHEKM Algorithm

---

**Require:**  $\mathbf{x}(n) = [x(n) \dots x(n - L + 1)]^T$ ,  $\mathbf{w}(n) = [w_0(n) \dots w_{L-1}(n)]^T$ **Require:**  $d(n), P(z), S(z)$ **Require:**  $\mu, \zeta, \eta, \alpha, p, \rho(1) = \mu$  and  $\phi(e(n)) = 0$ **while**  $n \leq L$  **do**

$$y(n) = \mathbf{x}(n)^T \mathbf{w}(n)$$

$$e(n) = d(n) - \mathbf{s}(n) * (\mathbf{w}(n)^T \mathbf{x}(n))$$

**if**  $e(n) < \zeta$  **then**

$$\mathbf{w}(n+1) = \mathbf{w}(n) + \mu \sum_{k=1}^N \rho^{N-k} \phi(e(n)) |e(n)|^{p-1} \mathbf{x}'(n)$$

**else**

$$\mathbf{w}(n+1) = \mathbf{w}(n)$$

**end if****end while**

---

the MSE of the proposed FXHEKM algorithm at steady state. To this end, we use the method of convergence evaluation to obtain the stability, stationary, and other critical aspects of the algorithm developed.

**3.3.1****Stability Evaluation**

Let us begin the analysis with the update Equation (3-6), where we subtract the optimal weights  $\mathbf{w}_o$  from both sides of the equation. Then, we obtain

$$\begin{aligned} \boldsymbol{\varepsilon}(n+1) &= \boldsymbol{\varepsilon}(n) + \mu \sum_{k=1}^N \rho^{N-k} \phi(e(n)) |e(n)|^{p-1} \mathbf{x}'(n) \\ &= \boldsymbol{\varepsilon}(n) + g(e(n)), \end{aligned} \quad (3-9)$$

where  $\boldsymbol{\varepsilon}(n)$  is the error of the filter weights at time  $n$  with respect to the optimal weight vector, in a similar form to Equation (2-14), *i.e.*  $\boldsymbol{\varepsilon}(n) = \mathbf{w}(n) - \mathbf{w}_o$ .

As we can observe, the term related to the hyperbolic secant of an exponential can be difficult to formulate in an analytical solution. Then, we consider as a boundary approximation the case of  $p = 2$  (standard form of FXHEKM).

Taking in the last equation the term referred to as  $g(e(n))$ , which is a function-related derivative, where we decouple the error to manipulate some steps that permit the stability analysis, we get

$$\begin{aligned}
g(e(n)) &= \mu \sum_{k=1}^N \rho^{N-k} q(e(n)) \operatorname{sech}^2 \left( \alpha \exp^{-\eta|e(n)|^2} \right) \exp^{-\eta|e(n)|^2} \frac{\operatorname{sign}(e(n))}{\|\mathbf{x}'(n)\|_2^2} \\
&\quad |d(n) - \mathbf{x}'(n)^H \mathbf{w}(n)| \mathbf{x}'(n) \\
&= \mu \sum_{k=1}^N \rho^{N-k} \phi(e(n)) |e_0^*(n) + \mathbf{w}_o^H \mathbf{x}'(n) - \mathbf{x}'(n)^H \mathbf{w}(n)| \mathbf{x}'(n) \\
&= \mu \sum_{k=1}^N \rho^{N-k} \phi(e(n)) (\mathbf{x}'(n) e_0^*(n) + \mathbf{x}'(n)^H \mathbf{x}'(n) (\mathbf{w}_o^H - \mathbf{w}(n))) \\
&= \mu \sum_{k=1}^N \rho^{N-k} \phi(e(n)) (\mathbf{x}'(n) e_0^*(n) + (\mathbf{x}'(n)^H \mathbf{x}'(n) \boldsymbol{\varepsilon}(n))).
\end{aligned} \tag{3-10}$$

Note that we consider here  $\delta = 0$  for the sake of simplicity. Returning to Equation 3-9, applying the expected value operator, and rearranging the terms, we have

$$\begin{aligned}
E[\boldsymbol{\varepsilon}(n+1)] &= \\
&E \left[ \left( \mathbf{I} - \left( \mu \sum_{k=1}^N \rho^{N-k} \phi(e(n)) \right) \mathbf{x}'(n)^H \mathbf{x}'(n) \right) \boldsymbol{\varepsilon}(n) \right] - \\
&E \left[ \left( \mu \sum_{n=1}^k \rho^{k-n} \phi(e(n)) \right) \mathbf{x}'(n) e_0(n) \right].
\end{aligned} \tag{3-11}$$

Now, we assume that  $\mathbf{x}'(n)$  is independent from  $\boldsymbol{\varepsilon}(n)$  and  $e_0(n)$ . Using this notion, we can get

$$E[\boldsymbol{\varepsilon}(n+1)] = \left( \mathbf{I} - \mu \sum_{k=1}^N \rho^{N-k} E[\phi(e(n))] \mathbf{R}_{\mathbf{x}'} \right) E[\boldsymbol{\varepsilon}(n)]. \tag{3-12}$$

Then, we can use the principle of the *eigenvalue decomposition* [45] method denoted by

$$\mathbf{R}_{\mathbf{x}'} = \mathbf{V} \boldsymbol{\Lambda} \mathbf{V}^H, \tag{3-13}$$

where  $\mathbf{V}$  is a unitary matrix, *i.e.*  $\mathbf{V}^H \mathbf{V} = \mathbf{V} \mathbf{V}^H = \mathbf{I}$  and  $\boldsymbol{\Lambda}$  is a diagonal matrix with the eigenvalues of  $\mathbf{R}_{\mathbf{x}'}$ . Thus, using the above expression in the update recursion of the weight error estimation, we obtain

$$E[\boldsymbol{\varepsilon}(n+1)] = \left( \mathbf{I} - \mu \sum_{k=1}^N \rho^{N-k} E[\phi(e(n))] \mathbf{V} \boldsymbol{\Lambda} \mathbf{V}^H \right) E[\boldsymbol{\varepsilon}(n)], \tag{3-14}$$

which is the nonlinear stochastic difference equation to the stability condition of the HEKM function. Multiplying both sides by the unitary matrix  $\mathbf{V}$  and rearranging the terms, we get

$$E[\boldsymbol{\varepsilon}'(n+1)] = \left( \mathbf{I} - \mu \sum_{k=1}^N \rho^{N-k} E[\phi(e(n))] \boldsymbol{\Lambda} \right) E[\boldsymbol{\varepsilon}'(n)]. \quad (3-15)$$

For the evaluation of the convergence of the recursion of the FXHEKM algorithm, we can rewrite the recursion step as

$$\begin{aligned} E[\boldsymbol{\varepsilon}'(3)] &= \left( \mathbf{I} - \mu \sum_{k=1}^N \rho^{N-k} E[\phi(e(2))] \boldsymbol{\Lambda} \right) E[\boldsymbol{\varepsilon}'(2)] \\ &= \left( \mathbf{I} - \mu \sum_{k=1}^N \rho^{N-k} E[\phi(e(1))] \boldsymbol{\Lambda} \right)^2 E[\boldsymbol{\varepsilon}'(1)]. \end{aligned} \quad (3-16)$$

Using this recursion to  $n = l$  elements, we obtain

$$E[\boldsymbol{\varepsilon}'(l+1)] = \left( \mathbf{I} - \mu \sum_{k=1}^N \rho^{N-k} E[\phi(e(l))] \boldsymbol{\Lambda} \right)^l E[\boldsymbol{\varepsilon}'(1)], \quad (3-17)$$

and taking into account the need to use only the diagonal elements, we can apply the decoupling property in the error weight vector. Therefore, we can obtain a simplified form for the  $k$ -th component of  $\boldsymbol{\varepsilon}'(n)$  given by

$$E[\boldsymbol{\varepsilon}'_k(n+1)] = \left( 1 - \mu \sum_{k=1}^N \rho^{N-k} E[\phi(e(n))] \boldsymbol{\lambda}_k \right)^{n+1} E[\boldsymbol{\varepsilon}'_k(0)], \quad (3-18)$$

where the expression above is function of the singular value  $\boldsymbol{\varepsilon}'_k(0)$ , and the  $\boldsymbol{\lambda}_k$  is the  $k$ -th component of  $\boldsymbol{\Lambda}$ . Then, analyzing the condition that guarantees convergence of the FXHEKM algorithm, the coefficients in the mean, we need to satisfy that

$$\left| 1 - \mu \sum_{k=1}^N \rho^{N-k} E[\phi(e(n))] \boldsymbol{\lambda}_k \right| < 1, \quad (3-19)$$

where the eigenvector  $\boldsymbol{\lambda}_k$  is the set of eigenvalues related to the autocorrelation matrix  $\mathbf{R}_x$  that solves the Wiener filter problem. Expanding the expression and

isolating the term of the step-size, we arrive at an expression for the stability condition given by

$$-1 < 1 - \mu \sum_{k=1}^N \rho^{N-k} E[\phi(e(n))] \boldsymbol{\lambda}_k < 1, \quad (3-20)$$

$$0 < \mu \sum_{k=1}^N \rho^{N-k} E[\phi(e(n))] \boldsymbol{\lambda}_k < 2, \quad (3-21)$$

and finally, we obtain that

$$0 < \kappa < \frac{2}{\boldsymbol{\lambda}_{max} \Phi(e(n))}, \quad (3-22)$$

where

$$\kappa = \mu \sum_{k=1}^N \rho^{N-k}, \quad (3-23)$$

is the alternative expression for the constant which controls the step of the learning curve and includes the value of the step-size and the forgetting factor, and

$$\begin{aligned} \Phi(e(n)) &= E[\phi(e(n))] \\ &= E\left[\left(\operatorname{sech}^2\left(\alpha \exp^{-\eta|e(n)|^p}\right) \exp^{-\eta|e(n)|^p} \frac{\operatorname{sign}(e(n))}{\delta + \|\mathbf{x}'(n)\|_2^2}\right)\right] \\ &\approx \frac{1}{N} \sum_{n=0}^{N-1} \left(\operatorname{sech}^2\left(\alpha \exp^{-\eta|e(n)|^p}\right) \exp^{-\eta|e(n)|^p} \frac{\operatorname{sign}(e(n))}{\delta + \|\mathbf{x}'(n)\|_2^2}\right), \end{aligned} \quad (3-24)$$

is the analytical expression that represents a function of the residual error defined by the expected value of a resulting component function of the FXHEKM algorithm, which is calculated in the learning process.

Lastly, we still have another alternative expression for the stability condition. In the case of  $p = 2$  (a special case of FXHEKM), we have

$$0 < \kappa < \frac{1}{\boldsymbol{\lambda}_{max} E\left[\left(\operatorname{sech}^2\left(\alpha \exp^{-\eta|e(n)|^2}\right) \exp^{-\eta|e(n)|^2} \frac{\operatorname{sign}(e(n))}{\|\mathbf{x}'(n)\|_2^2}\right)\right]}, \quad (3-25)$$

or the generalized form

$$0 < \mu < \frac{1}{\sum_{k=1}^N \rho^{N-k} \boldsymbol{\lambda}_{max} \Phi(e(n))}, \quad (3-26)$$

where the last is only related to the step-size value (as the classic literature denotation) of the FXHEKM algorithm.

In general, all of the three last equations represent different formulations to express the condition of the stability of the proposed algorithm. However, the term of the expected value of the derived expression, function  $\Phi(e(n))$  in (3-24), needs special attention to reach a satisfactory mathematical consistency.

### 3.3.2 Steady-state MSE

In this section, we analyze the update error function of the algorithm behavior at the moment when the stationary stage is reached (*vide* Section 2.3.2.3). Firstly, we employ the MSE objective function (2-38) that can be written as

$$\begin{aligned}
J(n) &= E \left[ |e(n)|^2 \right] \\
&= E \left[ (e_0(n) + \boldsymbol{\varepsilon}^H(n) \mathbf{x}'(n))^* (e_0(n) + \boldsymbol{\varepsilon}^H(n) \mathbf{x}'(n)) \right] \\
&= E [e_0(n)^* e_0(n)] + E [e_0(n)^* \boldsymbol{\varepsilon}^H(n) \mathbf{x}'(n)] \\
&\quad + E [e_0(n) \mathbf{x}'^H(n) \boldsymbol{\varepsilon}(n)] + E [\mathbf{x}'^H(n) \boldsymbol{\varepsilon}(n) \boldsymbol{\varepsilon}^H(n) \mathbf{x}'(n)].
\end{aligned} \tag{3-27}$$

As we know, we use the concept of the statistical independence from  $e_0(n)$  to  $\boldsymbol{\varepsilon}(n)$  and  $\mathbf{x}'$  [46]. Then, we obtain

$$\begin{aligned}
J(\infty) &= J_{\min} + J_{ex} \\
&= J_{\min} + \mathbf{tr}\{\mathbf{K}(n) \mathbf{R}'_x\} \\
&= J_{\min} + \mathbf{tr}\{\boldsymbol{\Lambda} \mathbf{U}\} \\
&= J_{\min} + \sum_{i=1}^M \lambda_i u_{i,i}(n),
\end{aligned} \tag{3-28}$$

is the function-based calculation of the excess value of the MSE estimation. Using Equations (2-39) for the function of the HEKM model term in (3-12), we get

$$J(\infty) = J_{\min} + \operatorname{tr} \left\{ \left( \mathbf{I} - \mu \sum_{k=1}^N \rho^{N-k} E[\phi(e(n))] \mathbf{R}'_x \right) \mathbf{K}(n-1) \left( \mathbf{I} - \mu \sum_{k=1}^N \rho^{N-k} E[\phi(e(n))] \mathbf{R}'_x \right) \right\}, \quad (3-29)$$

where the second term on the right side is the excess value of the MSE estimation, which is analogously the Equation (2-41). An important step here is the calculation of the covariance matrix of the weight error vector. From the definition of  $\mathbf{K}(n)$  and using (3-15), that expression is given by

$$\mathbf{K}(n+1) = E \left[ \boldsymbol{\varepsilon}(n+1) \boldsymbol{\varepsilon}^H(n+1) \right], \quad (3-30)$$

where extending the expression of the weight error vector, we have

$$\begin{aligned} \mathbf{K}(n+1) = & E \left[ \left( \mathbf{I} - \left( \mu \sum_{k=1}^N \rho^{N-k} \phi(e(n)) \right) \mathbf{x}'(n)^H \mathbf{x}'(n) \right) \boldsymbol{\varepsilon}(n) - \right. \\ & \left. \left( \mu \sum_{n=1}^k \rho^{k-n} \phi(e(n)) \right) \mathbf{x}'(n) e_0(n) \right] = \\ & E \left[ \left( \mathbf{I} - \left( \mu \sum_{k=1}^N \rho^{N-k} \phi(e(n)) \right) \mathbf{x}'(n)^H \mathbf{x}'(n) \right) \boldsymbol{\varepsilon}(n) - \right. \\ & \left. \left( \mu \sum_{n=1}^k \rho^{k-n} \phi(e(n)) \right) \mathbf{x}'(n) e_0(n) \right]^H \end{aligned} \quad (3-31)$$

and

$$\phi(e(n)) = \operatorname{sech}^2 \left( \alpha \exp^{-\eta|e(n)|^p} \right) \exp^{-\eta|e(n)|^p} \frac{\operatorname{sign}(e(n))}{\|\mathbf{x}'(n)\|_2^2}, \quad (3-32)$$

is an alternative simplified expression to recall the notation of the FXHEKM model in the mathematical analysis procedure. Organizing the terms, we get

$$\begin{aligned}
\mathbf{K}(n+1) = & \\
& E \left[ \left( \mathbf{I} - \left( \mu \sum_{k=1}^N \rho^{N-k} \phi(e(n)) \right) \mathbf{x}'(n) \mathbf{x}'(n)^H \right) \boldsymbol{\varepsilon}(n) \boldsymbol{\varepsilon}(n)^H \right. \\
& \quad \left. \left( \mathbf{I} - \left( \mu \sum_{k=1}^N \rho^{N-k} \phi(e(n)) \right)^* \mathbf{x}'(n) \mathbf{x}'(n)^H \right) \right] \\
& - E \left[ \left( \mathbf{I} - \left( \mu \sum_{k=1}^N \rho^{N-k} \phi(e(n)) \right) \mathbf{x}'(n) \mathbf{x}'(n)^H \right) \boldsymbol{\varepsilon}(n) \right. \\
& \quad \left. \left( \mu \sum_{n=1}^k \rho^{k-n} \phi(e(n)) \right) \mathbf{x}'(n)^H e_0(n) \right] \\
& - E \left[ \left( \mathbf{I} - \left( \mu \sum_{k=1}^N \rho^{N-k} \phi(e(n)) \right)^* \mathbf{x}'(n) \mathbf{x}'(n)^H \right) \boldsymbol{\varepsilon}(n)^H \right. \\
& \quad \left. \left( \mu \sum_{n=1}^k \rho^{k-n} \phi(e(n)) \right) \mathbf{x}'(n)^H e_0(n) \right] \\
& + E \left[ \left( \mu \sum_{k=1}^N \rho^{N-k} \right)^2 |\phi(e(n))|^2 |e_0(n)|^2 \mathbf{x}'(n) \mathbf{x}'(n)^H \right].
\end{aligned} \tag{3-33}$$

Using the known condition of statistical independence for  $e_0(n)$  and  $\boldsymbol{\varepsilon}(n)$ , and assuming the orthogonality principle between  $e_0(n)$  and  $\mathbf{x}'(n)$ , we arrive at the last equation divided in  $\mathbf{T}_i$  terms:

$$\begin{aligned}
\mathbf{T}_1 = & E \left[ \left( \boldsymbol{\varepsilon}(n) \boldsymbol{\varepsilon}(n)^H - \kappa \phi(e(n)) \mathbf{x}'(n) \mathbf{x}'(n)^H \boldsymbol{\varepsilon}(n) \boldsymbol{\varepsilon}(n)^H \right) \right. \\
& \quad \left. \left( \mathbf{I} - \kappa \phi(e(n))^* \mathbf{x}'(n) \mathbf{x}'(n)^H \right) \right] \\
= & \mathbf{K}(n) - \kappa E \left[ \phi(e(n)) \right] \mathbf{R}'_x \mathbf{K}(n) - \kappa E \left[ \phi(e(n)) \right] \mathbf{K}(n) \mathbf{R}'_x \\
& + \kappa^2 \mathbf{R}'_x \mathbf{K}(n) \mathbf{R}'_x \\
= & (\mathbf{I} - \kappa \mathbf{R}'_x \Phi(e(n))) \mathbf{K}(n) (\mathbf{I} - \kappa \mathbf{R}'_x \Phi(e(n))^*);
\end{aligned} \tag{3-34}$$

$$\mathbf{T}_2 = \mathbf{T}_3 = 0; \tag{3-35}$$

$$\begin{aligned}
\mathbf{T}_4 = & E \left[ \kappa^2 |\phi(e(n))|^2 |e_0(n)|^2 \mathbf{x}'(n) \mathbf{x}'(n)^H \right] \\
= & \kappa^2 |\Phi(e(n))|^2 J_{min} \mathbf{R}'_x.
\end{aligned} \tag{3-36}$$

Finally, we obtain for the covariance matrix expression that follows

$$\begin{aligned} \mathbf{K}(n+1) &= \left( \mathbf{I} - \kappa\Phi(e(n))\mathbf{R}'_x \right) \mathbf{K}(n) \left( \mathbf{I} - \kappa\Phi(e(n))\mathbf{R}'_x \right) \\ &\quad + \kappa^2|\Phi(e(n))^2|J_{min}\mathbf{R}'_x . \end{aligned} \quad (3-37)$$

Multiplying both sides by the unitary matrices  $\mathbf{V}$  and  $\mathbf{V}^H$  (Eq. (3-13)), we get

$$\begin{aligned} \mathbf{V}^H\mathbf{K}(n+1)\mathbf{V} &= \mathbf{V}^H \left( \mathbf{I} - \kappa\Phi(e(n))\mathbf{R}'_x \right) \mathbf{K}(n) \left( \mathbf{I} - \kappa\Phi(e(n))\mathbf{R}'_x \right) \mathbf{V} \\ &\quad + \kappa^2|\Phi(e(n))^2|J_{min}\mathbf{V}^H\mathbf{R}'_x\mathbf{V} . \end{aligned} \quad (3-38)$$

Then, simplifying the terms, we reach

$$\begin{aligned} \mathbf{U}(n+1) &= \left( \mathbf{V}^H - \kappa\Phi(e(n))\mathbf{\Lambda}\mathbf{V}^H \right) \mathbf{K}(n) \left( \mathbf{V} - \kappa\Phi(e(n))\mathbf{\Lambda}\mathbf{V} \right) \\ &\quad + \kappa^2|\Phi(e(n))^2|J_{min}\mathbf{\Lambda} . \end{aligned} \quad (3-39)$$

Therefore, the matrix  $\mathbf{U}(n+1)$  can be computed recursively as

$$\begin{aligned} \mathbf{U}(n+1) &= \left( \mathbf{I} - \kappa\Phi(e(n))\mathbf{\Lambda} \right) \mathbf{U}(n) \left( \mathbf{I} - \kappa\Phi(e(n))\mathbf{\Lambda} \right) \\ &\quad + \kappa^2|\Phi(e(n))^2|J_{min}\mathbf{\Lambda} . \end{aligned} \quad (3-40)$$

To calculate the excess MSE we need to diagonal elements of its matrices, which are described by

$$\mathbf{u}_{i,i}(n+1) = \left( 1 - \kappa^2\Phi(e(n))^2\lambda_i \right)^2 \mathbf{u}_{i,i}(n) + \kappa^2|\Phi(e(n))^2|J_{min}\lambda_i . \quad (3-41)$$

Based on Equation (3-41) and finding the expression of (3-28) to the stationary sense, now let us consider the performance of the HEKM algorithm at steady state. The diagonal elements are given by

$$\begin{aligned} \mathbf{u}_{i,i}(\infty) &= \left( 1 - \kappa^2\Phi(e(n))^2\lambda_i \right)^2 \mathbf{u}_{i,i}(\infty) + \kappa^2|\Phi(e(n))^2|J_{min}\lambda_i \\ &= \mathbf{u}_{i,i}(\infty) - 2\kappa^2\Phi(e(n))^2\lambda_i\mathbf{u}_{i,i}(\infty) + \kappa^4\Phi(e(n))^4\lambda_i^2\mathbf{u}_{i,i}(\infty) \\ &\quad + \kappa^2|\Phi(e(n))^2|J_{min}\lambda_i . \end{aligned} \quad (3-42)$$

Manipulating the equation products, arranging and simplifying the terms of the previous expression, we have

$$2\kappa^2\Phi(e(n))^2\lambda_i\mathbf{u}_{i,i}(\infty) - \kappa^4\Phi(e(n))^4\lambda_i^2\mathbf{u}_{i,i}(\infty) = \kappa^2|\Phi(e(n))^2|J_{\min}\lambda_i, \quad (3-43)$$

$$2\mathbf{u}_{i,i}(\infty) - \kappa^2\Phi(e(n))^2\lambda_i\mathbf{u}_{i,i}(\infty) = J_{\min}, \quad (3-44)$$

$$\mathbf{u}_{i,i}(\infty) (2 - \kappa^2\Phi(e(n))^2\lambda_i) = J_{\min}. \quad (3-45)$$

Therefore, we obtain that

$$\mathbf{u}_{i,i}(\infty) = \frac{J_{\min}}{2 - \kappa^2\Phi(e(n))^2\lambda_i}. \quad (3-46)$$

Thus, the excess MSE of the HEKM algorithm at steady-state is given by

$$J_{ex}(\infty) = J_{\min} \sum_{i=1}^M \frac{\lambda_i}{2 - \kappa^2\Phi(e(n))^2\lambda_i}. \quad (3-47)$$

At last, it interesting to point out the relation of misalignment of the adjustment factor, which can be formulated as

$$\mathcal{M} = \sum_{i=1}^M \frac{\lambda_i}{2 - \kappa^2\Phi(e(n))^2\lambda_i}, \quad (3-48)$$

and finally, returning to Equation (3-28), assuming that the algorithm will be in the steady state and applying the expression obtained in Equations (3-45)-(3-46), we have

$$\begin{aligned} J(\infty) &= J_{\min} (1 + \mathcal{M}) \\ &= J_{\min} \left( 1 + \sum_{i=1}^M \frac{\lambda_i}{2 - \kappa^2\Phi(e(n))^2\lambda_i} \right), \end{aligned} \quad (3-49)$$

where the formula of the steady-state MSE expression of the FXHEKM algorithm can be used to predict its MSE performance. Initially, we consider a standard simplification of

$$J_{\min} = \sigma_v^2, \quad (3-50)$$

as a reasonable value for the MMSE in the steady-state.

### 3.4 Numerical Results

In the present section, the performance of the proposed algorithm is compared with the classical and some robust methods via simulations. These methods, which employ the filtered-X framework, are: the FXLMS algorithm; the generalized Maximum Correntropy Criteria (FXGMCC) and its Improved version using the generalized Kernel (IFXGMCC) [21]; the generalized Hyperbolic Tangent function, *i.e.* GHT (FXGHT) algorithm [22], and an Exponential hyperbolic Cosine conjugated version (FXECH) algorithm [24]; the M-estimator algorithms (FXGR) [25] and the proposed FXHEKM algorithm.

Before the comparison of the proposed method against other approaches, an analysis of the HEKM function using different hyperbolic trigonometric formulations are realized in order to verify which is the most appropriate equation to model the proposed robust FXHEKM algorithm.

To evaluate the statistical analysis of this section with the practical values Figure 3.17 shows a comparison between the simulated curves of the state-of-the-art algorithms and the proposed FXHEKM algorithm against the analytical approach calculated in the last section.

#### 3.4.1 Computational Complexity

Using the update equation that describes the learning curve of the weight vector, we can compute the computational complexity in terms of arithmetic operations to compute the algorithms [47]. Table 3.1 shows the computational cost of several relevant algorithms [21,22,24,25], which are used as benchmarks in this thesis.

The variable  $L$  denote the length of the vector of the number of iterations,  $M$  is the filter tap length and  $p$  represent the power exponents used in some algorithms. In particular, the computational complexity is given in terms of arithmetic operations, *i.e.*, multiplications/divisions; sums and non-

linear operations such as  $\log(\cdot)$ ,  $\exp(\cdot)$ ,  $\text{sech}(\cdot)$  etc. Figure 3.8 illustrates the computational complexity against the filter length.

Table 3.1: Computation Complexity of some algorithms per iteration.

Algorithm	Mult , Div	+	Nonlinear Op
FXLMS	$2L+1$	$2L+2M-3$	-
FXGMCC	$2L+4$	$2L+2M-3$	3
FXGHT	$(p+5)(L-1) + L$	$3L-2$	1
IFXGMCC	$2L+6$	$2L+2M-3$	4
FXGR	$2L, 1$	$2L$	-
FXEHCF	$2L+p+8, 1$	$2L+2$	2
FXHEKM	$3L+2p+7, 1$	$3L-2$	4

Observing the number of mathematical operations in each method, the proposed FXHEKM algorithm has a slightly higher complexity than the other approaches, even in the number of multiplications and nonlinear operations (*e.g.*  $\tanh(\cdot)$ ,  $\exp(\cdot)$ ). However, this engineering trade-off is evaluated after the simulation analysis as follows.

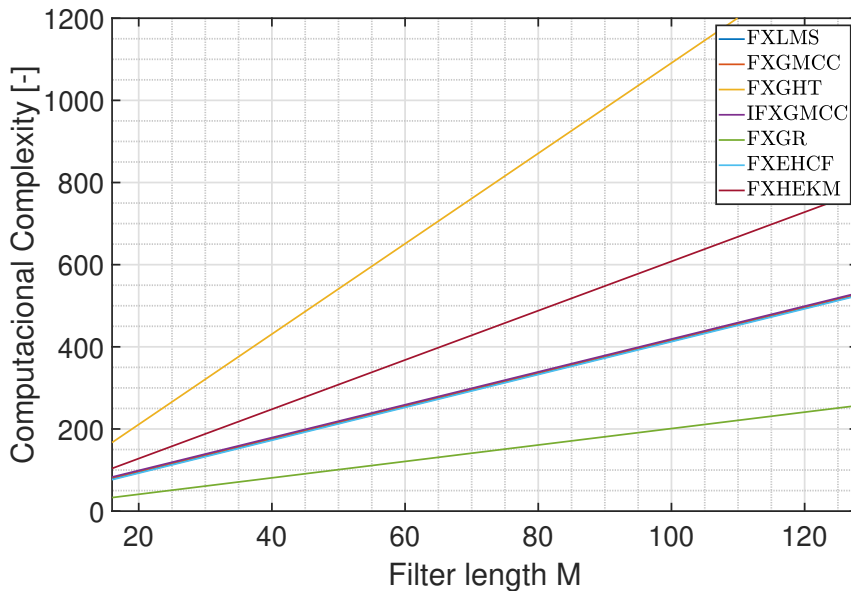


Figure 3.8: Computational Complexity of the algorithms approached.

It is noteworthy that although the methods improve the derivation of your math approach, its computational capacity needs to increase gradually (in

certain cases, this increase is nonlinear). The results regarding this engineering balance are shown in the next section.

### 3.4.2 Active Noise Cancellation of $\alpha$ -Stable Signals

To test the robustness of the algorithms the noise of the Gaussian and impulsive nature has been chosen as input in the validation procedure. The Gaussian noise is a standard test base, and the impulsive signal is an interesting special case with low probability but high amplitude variation and broad spectral content.

Based on the literature research, defined for this simulation focused in ANC the noise can be created by  $\alpha$ -Stable distribution [22] given by

$$\varpi(t) = \exp\{j\delta t - \gamma|t|^\alpha [1 + j\beta\text{sign}(t)S(t, \alpha)]\}, \quad (3-51)$$

where

$$S(t, \alpha) = \begin{cases} \frac{2}{\pi} \log |t|, & \text{if } \alpha = 1 \\ \tan(\frac{\alpha\pi}{2}), & \text{othersize} \end{cases}. \quad (3-52)$$

Here, the case study simulated the active noise cancellation in three scenarios considered:  $\alpha = 2.0$  (Gaussian noise) and 1.5 (pseudo-impulsive signal) in this study. The other three parameters are defined as standard  $\alpha$ -stable as  $\beta = 0$ ,  $\gamma = 1$  and  $\delta = 0$ . The input noise  $x(n)$  that follows an  $\alpha$ -stable distribution with  $\sigma_x^2 = 0.1$  – this value is chosen to standardize in both cases, in order to avoid extrapolating the peak values in case 2 (vide Figure 3.10). Finally, the variable  $v(n)$  is the independent measurement noise that follows a Gaussian random variable with zero mean and variance  $\sigma_v^2 = 0.001$ , or in other words, we set the measurement noise using a white noise with 1% of amplitude (*i.e.*  $0.01\text{randn}(L)$ ).

For the simulation procedure of the current work we used  $N = 15000$  iterations, filter length  $L = 16$ , and  $i = 250$  Monte Carlo simulations. The

impulsive responses used to primary path  $P(z) = 0.25z^{-2} + 0.5z^{-3} + 1.0z^{-4} + 0.5z^{-5} + 0.25z^{-6}$  and secondary path  $S(z) = 0.5P(z)$ .

A crucial step in filtered-X ANC systems is an estimation of the secondary path [48]. This is the main reason which justifies the use of the filtered-X approach, and at the same time that need for this kind of preliminary system identification task. In other words, an initial simulation is applied to define the initial values for the secondary path [49]. In the first scenario, Figure 3.9 shows the performance of the framework in the secondary path system identification.

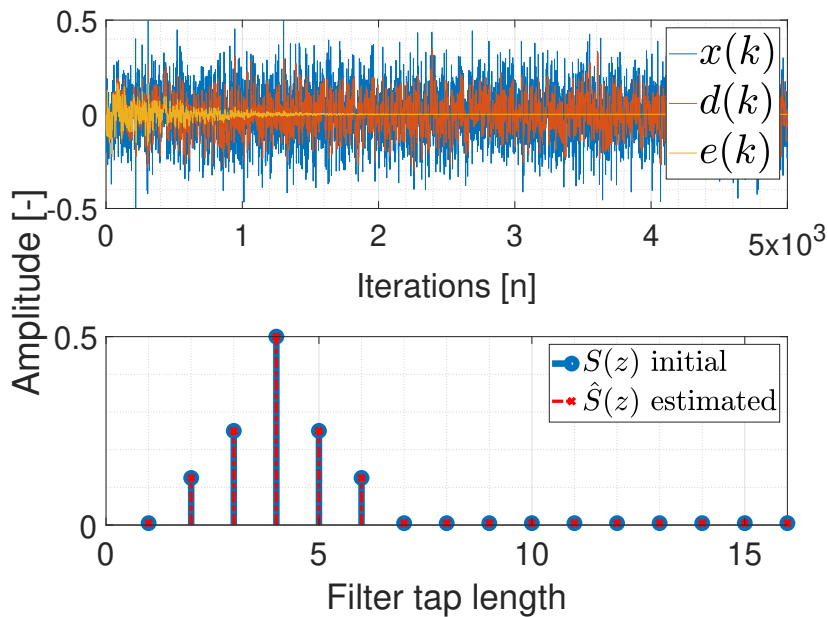


Figure 3.9: Analysis of the initial system identification realized to defined estimation of the secondary path  $\hat{S}(z)$  to  $\alpha = 2.0$  (case 1).

Similarly, Figure 3.10 shows an example with impulsive noise stability evaluation in the secondary path, where it is possible to observe the results are reaching a small error that indicates the effectiveness of the system in canceling the noise.

It is possible to note in the first graph above, the estimation of error (yellow line) decreasing and quickly reaching a value close to zero, which represents an efficient noise reduction. In the second graph, it is outstanding the precise filter estimation of the secondary path notes that the coincidental

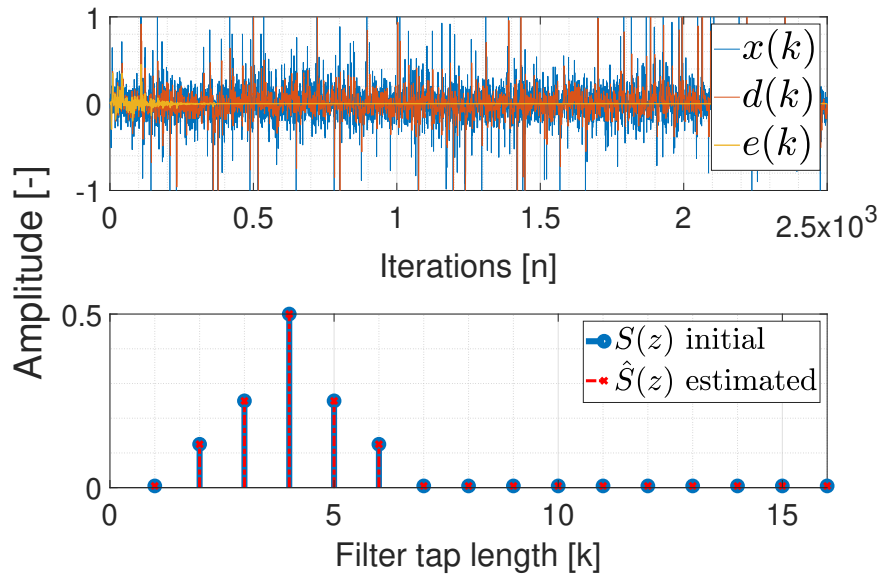


Figure 3.10: Analysis of the initial system identification realized to defined estimation of the secondary path  $\hat{S}(z)$  to  $\alpha = 1.5$  (case 2).

response value of the  $\hat{S}(z)$  and  $W(z)$ .

Moreover, the following analysis of the comparison between different methods related to your ANR performances is divided into two cases. The algorithm parameters are chosen after an exhaustive experimental procedure based on and respecting the convergence and stability analysis demonstrated previously in Section 2.3.

The values used in this case study for each method are FXLMS:  $\mu = 0.1$ ; FXGMCC:  $\mu = 0.0495$ ,  $\sigma = 1.5$ ,  $p = 1.7$  and  $\nu = 1.0$ ; FXGHT:  $\rho(1) = 0.1$ ,  $\lambda = 0.4$ ,  $p = 2$  and  $\sigma = 14.5$ ; IFXGMCC:  $\mu = 0.0535$ ,  $\sigma = 2.0$ ,  $p = 1.5$  and  $\nu = 0.5$ ; FXGR:  $\mu = 0.1$  and  $\zeta = 0.2$ ; FXECH:  $\gamma = \exp(1)$ ,  $\mu = 0.034$  and  $\lambda = 3.4$  and  $p = 2$ ; FXHEKM:  $\rho(1) = 0.1$ ,  $\eta = 1.0$ ,  $\alpha = 0.4$ ,  $\zeta = 0.2$  and  $p = 2.0$ . In Section 3.4.3 we bring all the results reached in the simulations as well as all highlights of the analysis and other important observations taken out.

### 3.4.3 MSE

The analysis of the obtained results on the estimation of the MSE is divided as: i) SNR comparison, where the statistical stability when the ratio

decrease are evaluated and ii) step-size comparison, where the value of  $\eta$  influences directly the behaviour of the learning curve of the HEKM function. These results are simulated first to evaluate the proposed methods in some different perspectives of its objective function, and later the best formulation against the other methods in the literature.

### 3.4.3.1 SNR Comparison

Firstly, a comparison related to the best approach used in the FXHEKM algorithm is performed. In Figure 3.11, it is possible to observe the evolution of the MSE over the iterations using SNR = 20 dB. Some simulations are sliced in a lower number of iterations when the stability condition are guaranteed, it only for effect of visualization improvement.

The comparison below is between the three versions, which each one using a different hyperbolic trigonometric expression in the objective function of the FXHEKM algorithm defined in Equation (3-3).

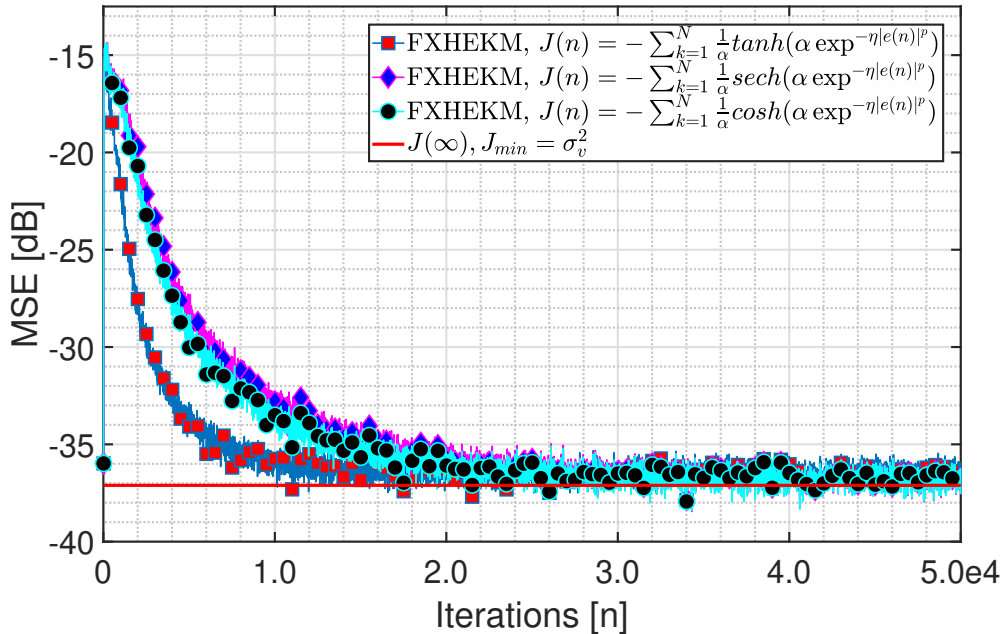


Figure 3.11: MSE comparison between HEKM method approaches for Gaussian distribution noise (SNR = 20 dB).

An important point to consider is that the method achieves the MMSE value of the theoretical calculation of (3-50), described in Section 3.3.2. Another interesting aspect for this simulation is that the algorithm using  $J(n)$  defined as (3-3) has the best performance according to the convergence and reaches the same value of MMSE.

Figure 3.12 shows an analogous simulation of the different HEKM approaches to the reduced value of the SNR. The results of MSE are close in performance among themselves, but the objective function using the  $\tanh(\cdot)$  in the term of the trigonometric function has the largest value around the mean.

A simulation example with other SNR values was also conducted. The main idea was to compare the influence of the relation between the input noise  $x(n)$  and the measurement additive noise  $v(n)$  inserted in the primary path. Finally, Figure 3.13 demonstrates the MSE evaluation in the last and worst case.

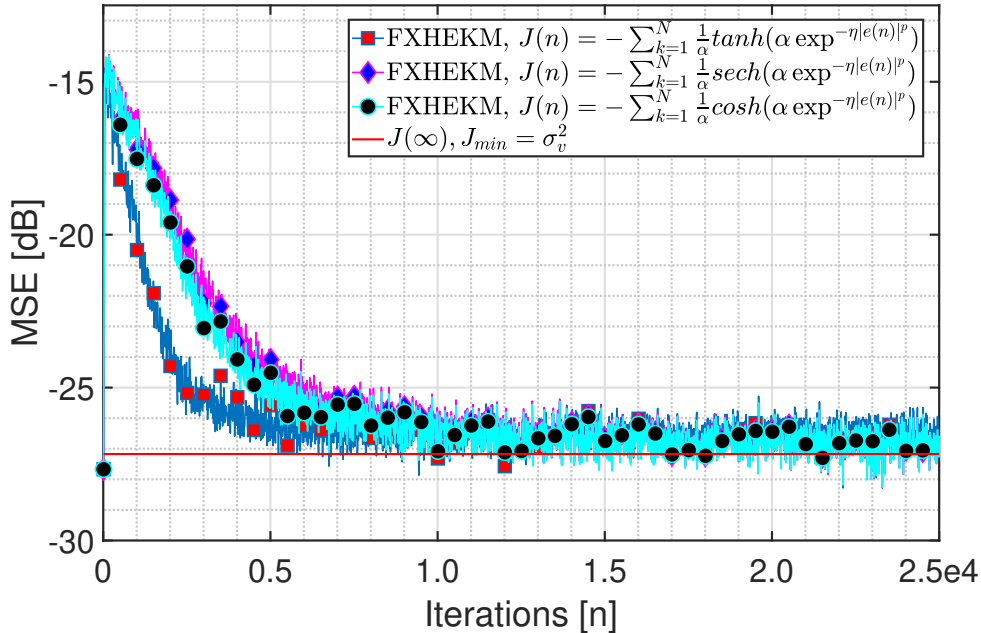


Figure 3.12: MSE comparison between HEKM method approaches for Gaussian distribution noise (SNR = 10 dB).

In the last SNR setting, the MSE of the standard version of the HEKM function around the mean and the MMSE increase dramatically as compared

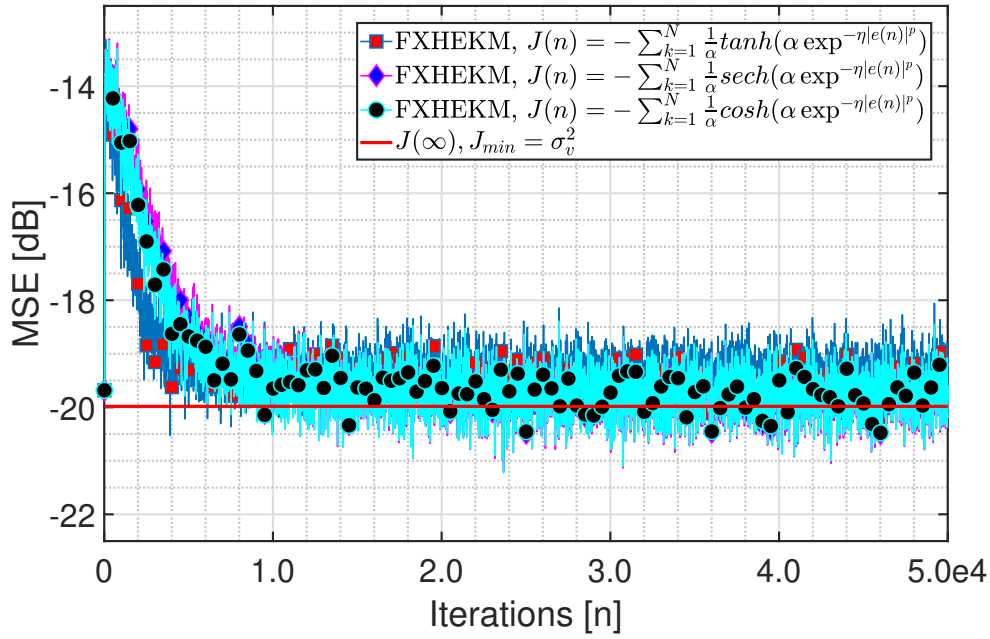


Figure 3.13: MSE comparison between HEKM method approaches for Gaussian distribution noise (SNR = 3 dB).

to the other version. Figure 3.14 shows the final value obtained for each SNR comparison for the FXHEKM using the standard version (e.g. Equation (3-3)).

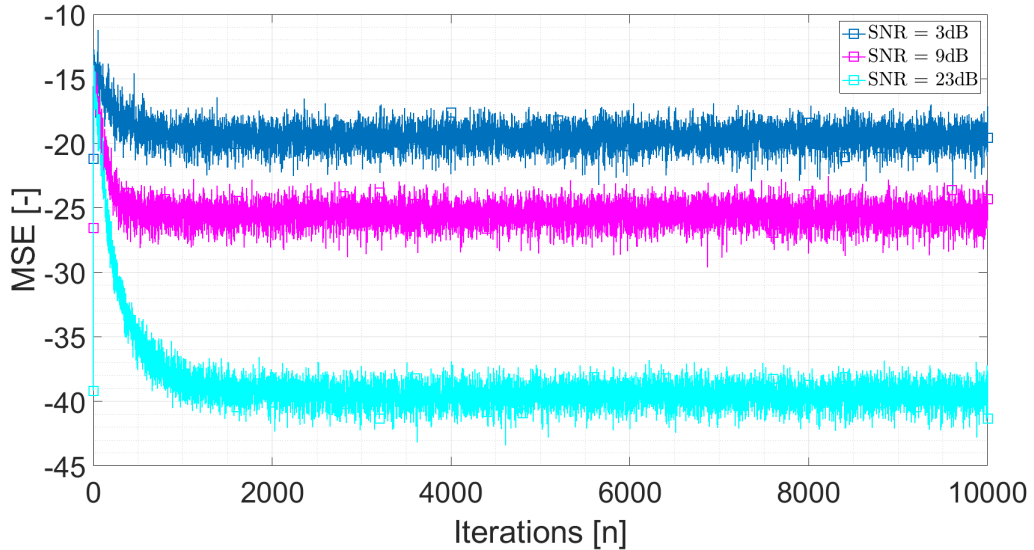


Figure 3.14: MSE analysis between different SNR values of the standard HEKM method for Gaussian distribution noise.

We can observe that the value between the beginning of the curve and the MMSE correspond to the exactly SNR applied.

### 3.4.3.2

#### $\eta$ Comparison

Here, we analyze the influence of the constant that controls the learning curve of the proposed model in terms of MSE estimation. To avoid the unnecessary repetition, a unique value are described and shown in the analysis above. Figure 3.15 illustrates the MSE comparison of the HEKM functions in the different hyperbolic trigonometric approaches to using the parameters  $\eta = 0.8$  (the fixed value of  $p = 2.0$ , then the step-size  $\mu = 1.6$ , with the forgetting factor  $\rho(N) \approx 1.25$ , therefore the constant  $\kappa \approx 2.0$ ).

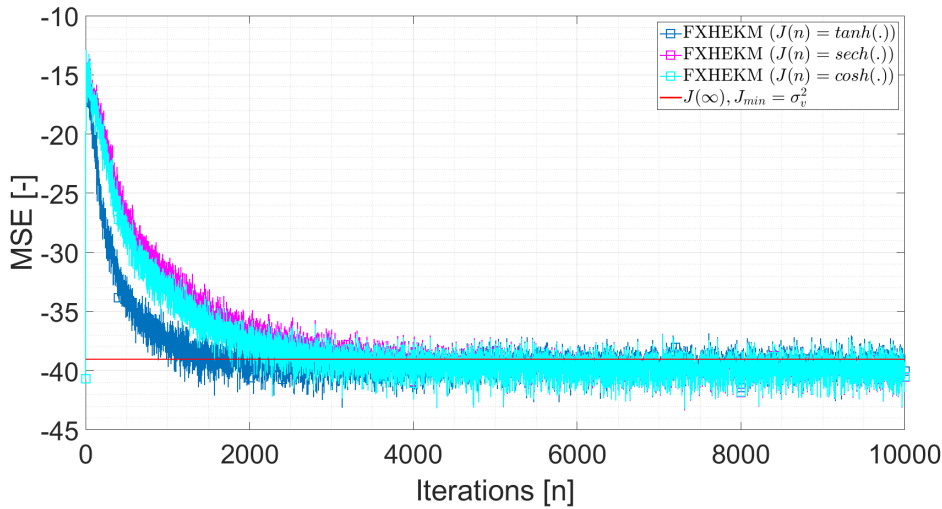


Figure 3.15: MSE comparison between HEKM method approaches for Gaussian distribution noise ( $\alpha - Stable = 2.0$ ).

To assess the evolution of the learning curve of the adaptive algorithms, the step-size is the most important parameter, and the performance trade-off. Therefore, Figure 3.16 shows the analysis of the relation between the parameter  $\eta$  and the MSE curves.

The results after some simulations get the notion of a optimal condition between quick convergence and lowest Minimum MSE estimation regarding the learning processing. For this reason the chosen value of  $\eta$  inside the step-size parameter is represented in the first curve ( $= 1.0$ ).

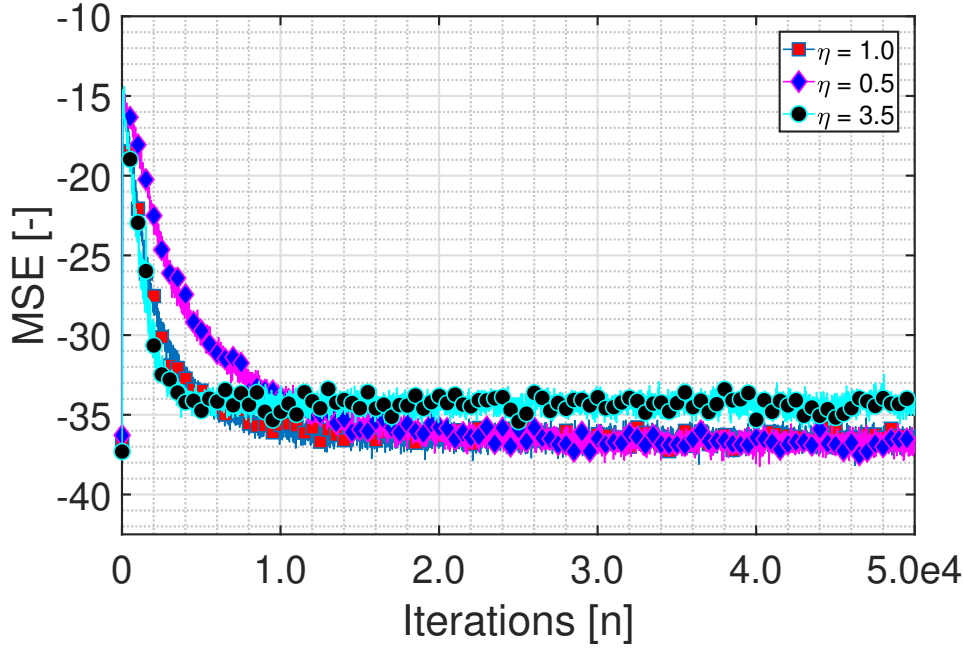


Figure 3.16: MSE comparison between HEKM method approaches for Gaussian distribution noise ( $\alpha - Stable = 2.0$ ).

### 3.4.3.3 Comparison of ANC Methods

For an SNR equal to 20 dB and the best settings of the step-size and parameters of the HEKM objective function, the Figure 3.17 brings the comparison between the FXHEKM algorithm and the other compared methods.

It is possible to visualize how the proposed FXHEKM algorithm has a faster convergence than other techniques, maintaining the stability than other classical and novel robust approaches.

In Section 3.4.4, we show an analysis of other chosen metric and their respective simulations realized to compare the methods studied in the work, evaluating the algorithm's performance and then concluding about the hypothesis raised.

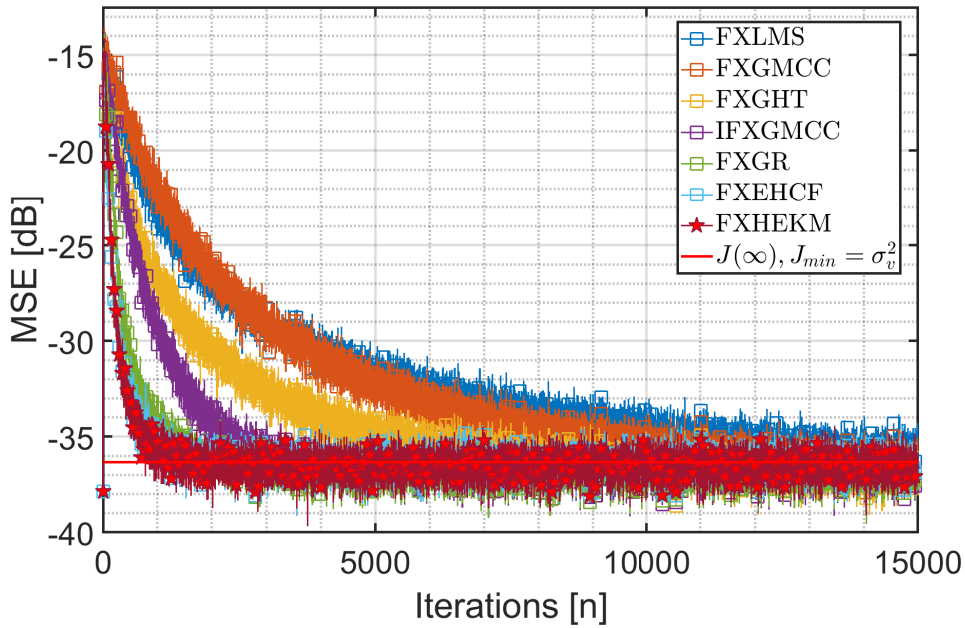


Figure 3.17: MSE comparison between HEKM method approaches for Gaussian distribution noise (SNR = 20 dB).

#### 3.4.4 ANR

In this subsection the noise cancellation performance of the ANC system is illustrated. For this purpose, the average noise reduction (ANR) is deployed as a metric [21]– [22], given by

$$\text{ANR}(n) = 20 \log \frac{A_{e(n)}}{A_{d(n)}}, \quad (3-53)$$

where  $A_{e(n)} = \theta A_{e(n-1)} + (1 - \theta)|e(n)|$ , with  $A_{e(0)} = 0$  denote the estimate of residual error;  $A_{d(n)} = \theta A_{d(n-1)} + (1 - \theta)|d(n)|$ , with  $A_{d(0)} = 0$  describe the estimate of the noise in primary path, and  $\theta = 0.99$  is the forgetting factor.

Here, we evaluated the ANC performance in two different scenarios: i) Gaussian signals ( $\alpha$ -Stable distribution = 2.0) and ii) Non-Gaussian or Impulsive signals ( $\alpha$ -Stable distribution = 1.5). In the first round of simulations, Figures 3.18 to 3.20 the 3 different levels of SNR are tested to verify the convergence speed and stability to the three analyzed versions of the FXHEKM algorithm.

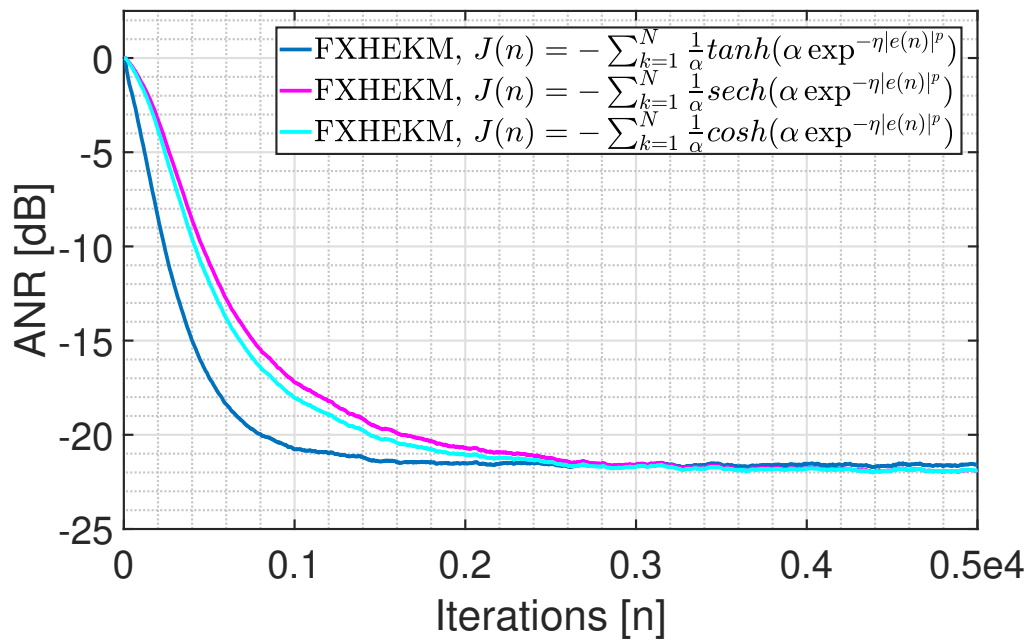


Figure 3.18: ANR comparison between HEKM approaches for Gaussian distribution noise (SNR = 20 dB).

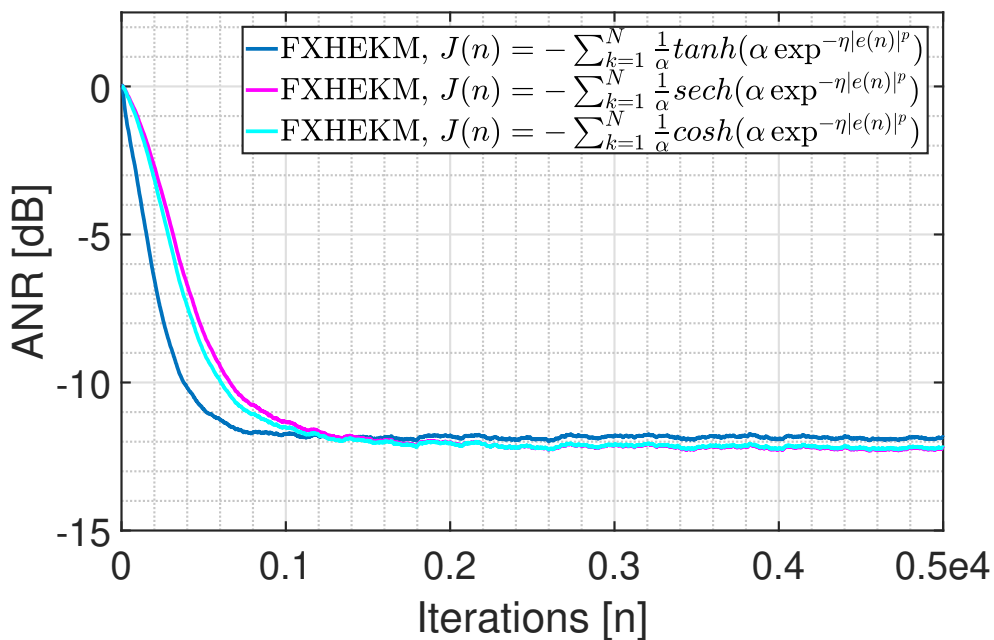


Figure 3.19: ANR comparison between HEKM method approaches for Gaussian distribution noise (SNR = 10 dB).

Some important points to observe include the curve using the hyperbolic tangent as part of its objective function reaches the fastest convergence speed

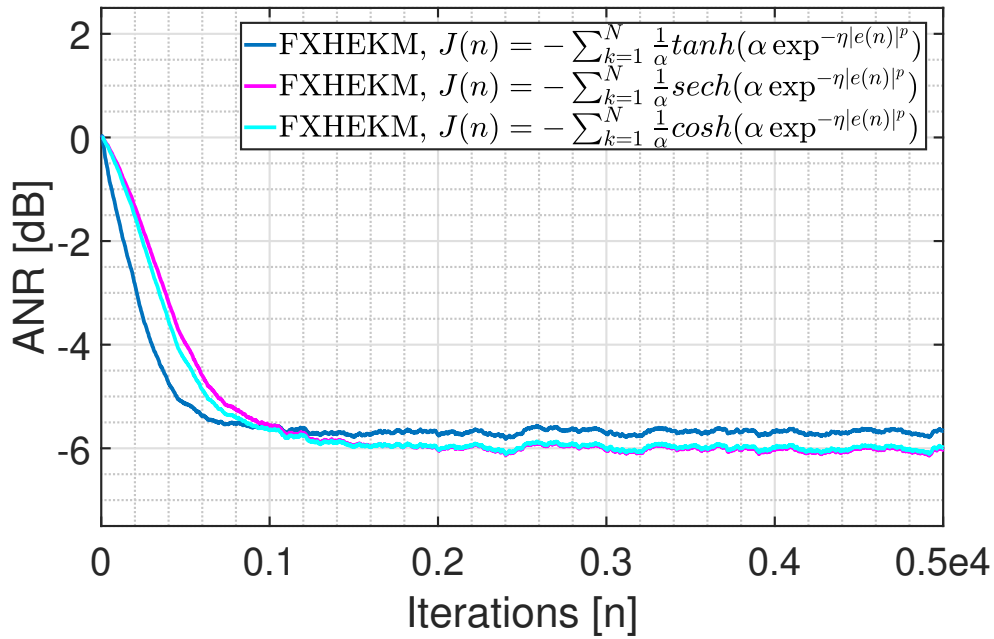


Figure 3.20: ANR comparison between HEKM method approaches for Gaussian distribution noise (SNR = 3 dB).

with comparable stability to other expressions. However, there is a trade-off between convergence speed and stability or Minimum MSE level [50]. This is a well-known relationship in adaptive algorithms [6], and here it is noteworthy that in extreme cases (SNR = 3 dB), the steady-state stage of the standard HEKM results in an increase in MSE of  $\approx 0.5$  dB.

A comparison of the ANR performance of the FXHEKM algorithm against all other studied methods is shown in Figure 3.21.

The simulation performed to set the parameters of all methods confirm the hypothesis presented about the performance of the proposed FXHEKM algorithm. As shown in the plot, the FXHEKM algorithm reaches the best performance, outperforming the other methods.

The analysis of ANR performance evaluates the proposed ANC framework in the presence of non-Gaussian noise. The idea to evaluate the impulsive noise is based on a range of practical problems [5]. For this numerical simulation, we employ the  $\alpha$ -Stable distribution noise = 1.5, which contains a signal with impulsive peaks mixed with some Gaussian distortion, as shown in Figure

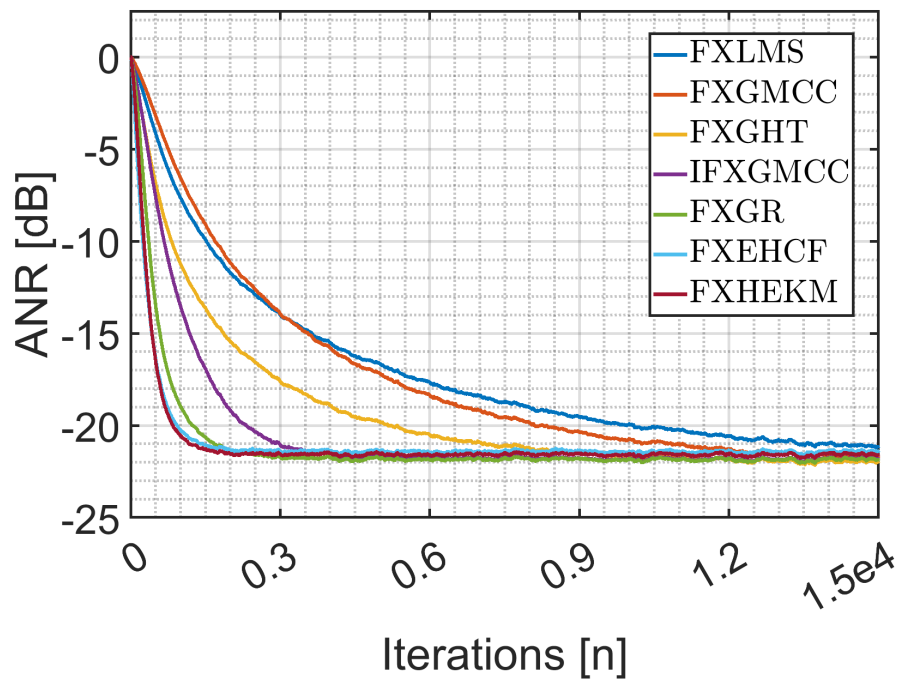


Figure 3.21: ANR comparison between HEKM method against other classical/robust approaches for Gaussian distribution noise (SNR = 20 dB).

3.10 with the same parameters and conditions used in the first scenario. Figure 3.22 shows the comparison between the versions of the FXHEKM algorithm.

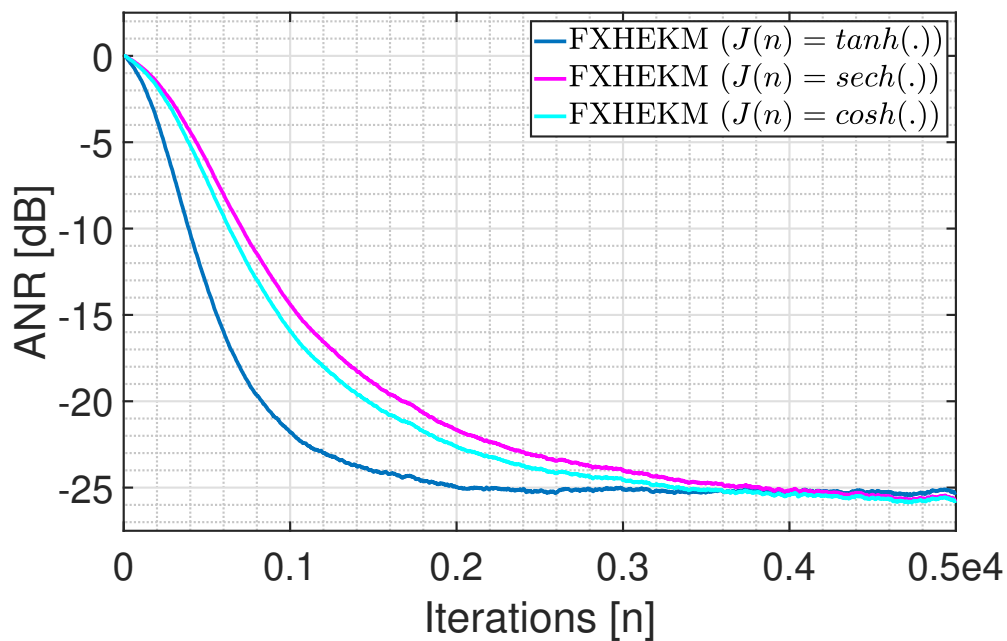


Figure 3.22: ANR comparison between HEKM approaches for impulsive noise (SNR  $\approx$  25dB).

As observed in the simulations using Gaussian noise, the HEKM function using the  $\tanh(\cdot)$  as a component term of the objective function obtained the best performance in convergence speed with the same MSE at steady state, overcoming the other approaches applied [22, 23].

A important point of this research in the algorithm development is the hypothesis to create a method able to deal with robustness against signals with non-Gaussian behaviour (e.g. white noise). After a second extensive round of simulations, adjusting the parameters and testing the algorithm's execution, we can observe a comparison of the methods in Figure 3.23.

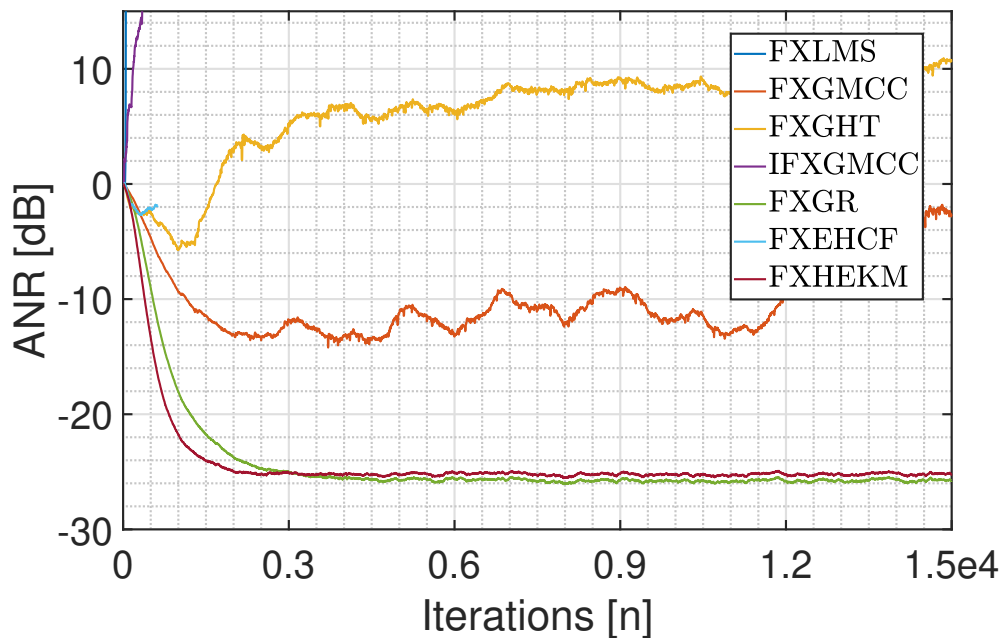


Figure 3.23: ANR comparison between HEKM method against other classical/robust approaches for Gaussian distribution noise ( $\text{SNR} \approx 25\text{dB}$ ).

The FXHEKM algorithm shows stability and fast convergence as well as adaptability to different scenarios of ANC. Indeed, the proposed FXHEKM algorithm outperforms the other algorithms in the scenarios studied.

### 3.4.5 Summary

This chapter brought the development of the mathematical approach, in the analytical and statistical sense, of the proposed FXHEKM algorithm. The

performance of the proposed FXHEKM algorithm using several metrics has been evaluated and shown that the FXHEKM outperforms recent competing techniques in the literature.

## 4

### Conclusions and Future Work

In this chapter, we draw the conclusions of this work along with a brief discussion of ideas for future work. This work investigated and developed robust adaptive filtering techniques for active noise cancellation. In particular, a new high performance approach using a robust objective function and an adaptive filtered-X framework in an ANC system have been devised. In order to study the performance of the proposed approach and obtain insights on its behaviour, a statistical analysis has been carried out and simulations were performed to understand the limitations of the proposed algorithm.

The performance of the proposed FXHEKM algorithm was evaluated using simulations and analytical expressions derived to predict the performance of the proposed algorithm. We have chosen to use the  $\alpha - Stable$  distribution signals for the broad used in the literature and the possibility to simulate a nice range of the different signals with the same variable. In this sense, we can conclude that the MSE analysis of the convergence and stability reinforces the study of the statistical behavior of the proposed algorithm against the classical and recent robust approaches in the literature. In all the scenarios simulated, we have the proposed FXHEKM algorithm reaching the MMSE value theoretically calculated in this work and overcoming all the other compared methods, which evidence the robustness against impulsive noise and effective performance.

In the case of signals in the presence of white noise ( $\alpha = 2.0$  that is analogous to Gaussian random signal), the FXHEKM algorithm outperforms all the methods, achieving the best value in the average noise reduction metric. In the second scenario in the presence of impulsive noise ( $\alpha = 1.5$  that consists of pseudo-impulsive noise), the results of the FXHEKM algorithm is held, being closely followed by the M-estimator method FXGR, confirming the

effectiveness to process signals with non-Gaussian nature. After exhaustive simulations, the proposed approach maintains the stability against the other robust models and surpasses the FXGR on average about 2-3dB until two thousand iterations.

For the future works, we have observed the results and the behavior of the proposed FXHEKM algorithm and would like to point out some possible following researches. Firstly, it would be interesting analyze some condition related to the proposed approach as the more deep analytical study about the Equations (3-24) and (3-26), and the band of convergence and stability in the threshold of (3-8); other simulation scenarios like other model (Auto Regressive, chaotic, real case), different input signal (real signals) or with other additive noise (types and SNR's) etc. It would be interesting to compare the proposed FXHEKM algorithm with other approaches that employ different optimization methods, affine projection and subband frameworks, machine learning and deep learning algorithms.

Further improvements in the way of this research might involve testing other types of noises (*i.e.* chaotic signals, real case signals), different systems and cases of applications (problems *e.g.* system identification, room equalization, denoising etc, or real-world applications, *e.g.* DSP issues, communication systems, acoustics and other specific fields like headphones and hearing aids, automotive, aeronautics, railway infrastructure etc) and some methodological improvements in kernel adaptive filtering approaches.

## 5

### Bibliography

- [1] OLSON, H. Electronic control of noise, vibration, and reverberation. *The Journal of The Acoustical Society of America*, The Journal of The Acoustical Society of America, v. 28, n. 5, 1956.
- [2] WIDROW, B. et al. Adaptive noise cancelling: Principles and applications. *Proceedings of the IEEE*, v. 63, n. 12, p. 1692–1716, 1975.
- [3] ELLIOTT, S.; STOTHERS, I.; NELSON, P. A multiple error lms algorithm and its application to the active control of sound and vibration. *IEEE Transactions on Acoustics, Speech, and Signal Processing*, v. 35, n. 10, p. 1423–1434, 1987.
- [4] BURGESS, J. C. Active adaptive sound control in a duct: A computer simulation. *The Journal of the Acoustical Society of America*, v. 70, n. 3, p. 715–726, 1981.
- [5] VASEGHI, S. V. *Advanced Digital Signal Processing and Noise Reduction*. [S.I.]: Wiley, 2008.
- [6] HAYKIN, S. *Adaptive Filter Theory*. [S.I.]: John Wiley & Sons, 1986. (Wiley series in telecommunications and signal processing).
- [7] WIDROW, B.; STEARNS, S. *Adaptive Signal Processing*. [S.I.]: Prentice Hall, 1985. (Prentice Hall Signal Processing Series).
- [8] KUO, S.; MORGAN, D. Active noise control: a tutorial review. *Proceedings of the IEEE*, v. 87, n. 6, p. 943–973, 1999.
- [9] NELSON, P.; ELLIOTT, S. *Active Control of Sound*. [S.I.]: Academic Press, 1992.
- [10] WIDROW, B. et al. Adaptive noise cancelling: Principles and applications. *Proceedings of the IEEE*, v. 63, n. 12, p. 1692–1716, 1975.

- [11] BJARNASON, E. Analysis of the filtered-x lms algorithm. *IEEE Transactions on Speech and Audio Processing*, v. 3, n. 6, p. 504–514, 1995.
- [12] LU, L. et al. A survey on active noise control in the past decade—part I: Linear systems. *Signal Processing*, v. 183, 2021.
- [13] LU, L. et al. A survey on active noise control in the past decade—part II: Nonlinear systems. *Signal Processing*, v. 181, 2021.
- [14] HUANG, B. et al. A variable step-size fxlms algorithm for narrowband active noise control. *IEEE Transactions on Audio, Speech, and Language Processing*, v. 21, n. 2, p. 301–312, 2013.
- [15] ZEB, A. et al. Improving performance of fxrls algorithm for active noise control of impulsive noise. *Applied Acoustics*, v. 116, p. 364–374, 2017. ISSN 0003-682X.
- [16] AKHTAR, M. T.; MITSUHASHI, W. Improving robustness of filtered-x least mean p-power algorithm for active attenuation of standard symmetric- $\alpha$ -stable impulsive noise. *Applied Acoustics*, v. 72, n. 9, p. 688–694, 2011.
- [17] ROUT, N. K.; DAS, D. P.; PANDA, G. Particle swarm optimization based nonlinear active noise control under saturation nonlinearity. *Applied Soft Computing*, v. 41, p. 275–289, 2016.
- [18] MORGAN, D. An analysis of multiple correlation cancellation loops with a filter in the auxiliary path. *IEEE Transactions on Acoustics, Speech, and Signal Processing*, v. 28, n. 4, p. 454–467, 1980.
- [19] ASLAM, M. S.; SHI, P.; LIM, C.-C. Variable threshold-based selective updating algorithms in feed-forward active noise control systems. *IEEE Transactions on Circuits and Systems I: Regular Papers*, v. 66, n. 2, p. 782–795, 2019.
- [20] LIU, W.; PRINCIPE, J. C.; HAYKIN, S. *Kernel Adaptive Filter - A Comprehensive Introduction*. [S.l.]: Wiley, 2010.

- [21] CHIEN, Y.-R.; YU, C.-H.; TSAO, H.-W. Affine-projection-like maximum correntropy criteria algorithm for robust active noise control. *IEEE/ACM Transactions on Audio, Speech, and Language Processing*, v. 30, p. 2255–2266, 2022.
- [22] XIAO, Y. et al. Generalized hyperbolic tangent based random fourier conjugate gradient filter for nonlinear active noise control. *IEEE/ACM Transactions on Audio, Speech, and Language Processing*, v. 31, p. 619–632, 2023.
- [23] ZHU, Y. et al. Cascaded random fourier filter for robust nonlinear active noise control. *IEEE/ACM Transactions on Audio, Speech, and Language Processing*, v. 30, p. 2188–2200, 2022.
- [24] KUMAR, K. et al. Exponential hyperbolic cosine robust adaptive filters for audio signal processing. *IEEE Signal Processing Letters*, v. 28, p. 1410–1414, 2021.
- [25] YU, Y. et al. General robust subband adaptive filtering: Algorithms and applications. *IEEE/ACM Transactions on Audio, Speech, and Language Processing*, v. 30, p. 2128–2140, 2022.
- [26] MORALES, L. G. *Adaptive Filtering*. [S.I.]: IntechOpen, 2013.
- [27] NELSON, P. A.; ELLIOTT, S. J. *Active Control of Sound*. [S.I.]: Academic Press, 1992.
- [28] KUO, S. M.; MORGAN, D. R. *Active Noise Control systems: algorithms and DSP implementations*. [S.I.]: John Wiley & Sons, 1996. (Wiley series in telecommunications and signal processing).
- [29] PAUL, L. Process of silencing sound oscillations. n. 2043416, June 1936. Disponível em: <<https://www.freepatentsonline.com/2043416.html>>.
- [30] OLSON, H. F. Electronic Control of Noise, Vibration, and Reverberation. *The Journal of the Acoustical Society of America*, v. 28, p. 156–156, 01 1956.

- [31] WIDROW, B.; LEHR, M. 30 years of adaptive neural networks: perceptron, madaline, and backpropagation. *Proceedings of the IEEE*, v. 78, n. 9, p. 1415–1442, 1990.
- [32] LAMARE, R. C. de; SAMPAIO-NETO, R. Adaptive reduced-rank processing based on joint and iterative interpolation, decimation, and filtering. *IEEE Transactions on Signal Processing*, v. 57, n. 7, p. 2503–2514, 2009.
- [33] SHENOI, B. A. *Introduction to Digital Signal Processing and Filtering Design*. [S.l.]: Wiley-Interscience, 2006. 423 p.
- [34] DINIZ, P. S. R. *Adaptive Filtering: Algorithms and Practical Implementation*. [S.l.]: Springer, 2020.
- [35] CHU, Y. et al. A new diffusion filtered-x affine projection algorithm: Performance analysis and application in windy environment. *IEEE/ACM Transactions on Audio, Speech, and Language Processing*, v. 32, p. 1596–1608, 2024.
- [36] HUYNH, M.-C.; CHANG, C.-Y. Novel adaptive fuzzy feedback neural network controller for narrowband active noise control system. *IEEE Access*, v. 10, p. 41740–41747, 2022.
- [37] YIN, K.-L.; PU, Y.-F.; LU, L. Robust q-gradient subband adaptive filter for nonlinear active noise control. *IEEE/ACM Transactions on Audio, Speech, and Language Processing*, v. 29, p. 2741–2752, 2021.
- [38] CHU, Y. et al. A new diffusion filtered-x affine projection algorithm: Performance analysis and application in windy environment. *IEEE/ACM Transactions on Audio, Speech, and Language Processing*, v. 32, p. 1596–1608, 2024.
- [39] GE, Q.; BAI, X.; ZENG, P. Gaussian-cauchy mixture kernel function based maximum correntropy kalman filter for linear non-gaussian systems. *IEEE Transactions on Signal Processing*, p. 1–14, 2024.

- [40] YIN, K.-L.; PU, Y.-F.; LU, L. Robust q-gradient subband adaptive filter for nonlinear active noise control. *IEEE/ACM Transactions on Audio, Speech, and Language Processing*, v. 29, p. 2741–2752, 2021.
- [41] LIU, T. et al. Joint estimation of doa and range for near-field sources in the presence of far-field sources and alpha-stable noise. *IEEE Signal Processing Letters*, v. 31, p. 406–410, 2024.
- [42] LU, L. et al. A survey on active noise control in the past decade—part II: Nonlinear systems. *Signal Processing*, v. 181, 2021.
- [43] YANG F.; GUO, J.; YANG, J. Stochastic analysis of the filtered-x lms algorithm for active noise control. *IEEE/ACM Transactions on Audio, Speech, and Language Processing*, ACM/IEEE, v. 28, p. 2252–2266, 2020.
- [44] BOYD, S.; VANDENBERGHE, L. *Convex Optimization*. [S.I.]: Cambridge University Press, 2004.
- [45] STRANG, G. *Introduction to Linear Algebra*. 6. ed. [S.I.]: CUP, 2023.
- [46] HAYES, M. H. *Statistical Digital Signal Processing and Modeling*. 1st. ed. USA: John Wiley & Sons, Inc., 1996. ISBN 0471594318.
- [47] SAYED, A. H. *Adaptive Filters*. [S.I.]: Wiley, 2008.
- [48] KUO, S.; VIJAYAN, D. A secondary path modeling technique for active noise control systems. *IEEE Transactions on Speech and Audio Processing*, v. 5, n. 4, p. 374–377, 1997.
- [49] CHANG, C.-Y.; S.M., K.; HUANG, C.-W. Secondary path modeling for narrowband active noise control systems. *Applied Acoustics*, v. 131, 2018.
- [50] BERSHAD, N. J.; BERMUDEZ, J. C. A switched variable step size nlms adaptive filter. *Digital Signal Processing*, v. 101, p. 102730, 2020.